Petrogenesis and geodynamic evolution of the Late Neoproterozoic post-collisional felsic magmatism in NE Afyon area, western central Turkey

S. Gürsu and M. C. Goncuoglu

Geological Society, London, Special Publications 2008; v. 297; p. 409-431
doi:10.1144/SP297.19

Petrogenesis and geodynamic evolution of the Late Neoproterozoic post-collisional felsic magmatism in NE Afyon area, western central Turkey

S. GÜRSU[1] & M. C. GONCUOGLU[2]

[1]*Natural History Museum, Mineralogy–Petrography Division, MTA, 06520, Ankara, Turkey (e-mail: semihgursu@yahoo.com)*

[2]*Department of Geological Engineering, Middle East Technical University, 06531, Ankara, Turkey*

Abstract: In western Turkey, Late Neoproterozoic basement rocks are represented by variably deformed metasedimentary and meta-igneous rocks within different tectonostratigraphical units that make up the Alpine Tauride–Anatolide Platform. In the Kütahya–Bolkar Dagı unit to the NE of Afyon this basement mainly includes garnet-bearing mica schists intruded by metamorphic granitic rocks with relict porphyritic textures. The youngest zircon ages obtained from the granitic rocks by the single zircon evaporation method are 542 $\pm$ 5.0 Ma on average, which correlate with the Late Pan-African–Cadomian granitic magmatism. The granitic rocks are rhyodacitic or dacitic and peraluminous in composition, and display geochemical characteristics of I-type (tonalite–trondhjemite–granodiorite (TTG) source) felsic intrusive rocks. Trace and rare earth element patterns with distinct depletion in Rb, K, Nb, Sr, P and Ti relative to the other trace elements correlate very well with a Proterozoic TTG source. The petrogenetic modelling also implies that they were developed by partial melting of a TTG source by 20% fractional melting plus 20% Rayleigh fractional crystallization. The emplacement temperatures estimated by using zircon (790–820 °C), apatite and monazite saturation thermometry are about 827–1035 °C; these are in accordance with I-type rather than S-type granite melts. A geochemical comparison of the NE Afyon granitic rocks with the coeval quartz-porphyries in the Sandikli area of the Geyik Dag tectonic unit suggests that the latter may represent the more evolved felsic part of the Cadomian magmatism. Hence, both basement complexes are parts of the same Gondwanan terrane and represent the eastern continuation of the North African–Southern European terrane assemblage.

A number of Precambrian terranes or microplates, named the Peri-Gondwanan terranes, are widespread in Southern Europe and the Eastern Mediterranean along the northern continental margin of West Gondwana (Amazonia and West Africa). They were separated from North Africa by the opening of several oceanic seaways known as Iapetus and Proto-, Palaeo- or Neotethys. The Tauride–Anatolide Platform in Turkey is one of the Cadomian-type Peri-Gondwanan terranes that formed along the West African margin by recycling of ancient West African crust (e.g. Murphy *et al.* 2002, 2004; Neubauer 2002) and had drifted from North Africa by the Early Mesozoic opening of the Bitlis–Zagros Neotethyan oceanic branch. The Alpine closure of this ocean resulted in a redistribution of the Late Neoproterozoic–Palaeozoic basement rocks and their Mesozoic cover within numerous allochthonous tectonostratigraphical units in eastern, central and southern Turkey. The Late Neoproterozoic basement rocks in these units are represented by diverse lithologies, including high-grade metamorphic complexes (e.g. basement of Menderes Massif, Dora *et al.* 1995; Candan *et al.* 2001), very low-grade metavolcanic assemblages (Gürsu & Goncuoglu 2001; Gürsu *et al.* 2004*a*, *b*) and sedimentary–volcanic successions (Kozlu & Goncuoglu 1997; Goncuoglu *et al.* 1997). The radiometric age data from the felsic igneous rocks range around *c*. 541–545 Ma, which correlates well with the Late Pan-African–Cadomian granitoids in North Africa and Gondwana-derived terranes in Southern and Central Europe (Ballèvre *et al.* 2001; Chantraine *et al.* 2001; El-Nisr *et al.* 2001; Pin *et al.* 2002; Bandres *et al.* 2002; Dörr *et al.* 2002; Genna *et al.* 2002; Mushkin *et al.* 2003) in terms of age and geochemistry. In the western central Taurides these basement rocks mainly occur within two main tectonic units (Fig. 1, distribution of Late Neoproterozoic basement rocks in western Anatolia). These are the Kütahya–Bolkar Dagı (NE of Afyon) and Geyik Dag (SW of Afyon) units, as reported by Goncuoglu & Kozlu (2000).

From: ENNIH, N. & LIÉGEOIS, J.-P. (eds) *The Boundaries of the West African Craton.* Geological Society, London, Special Publications, **297**, 409–431.
DOI: 10.1144/SP297.19 0305-8719/08/$15.00

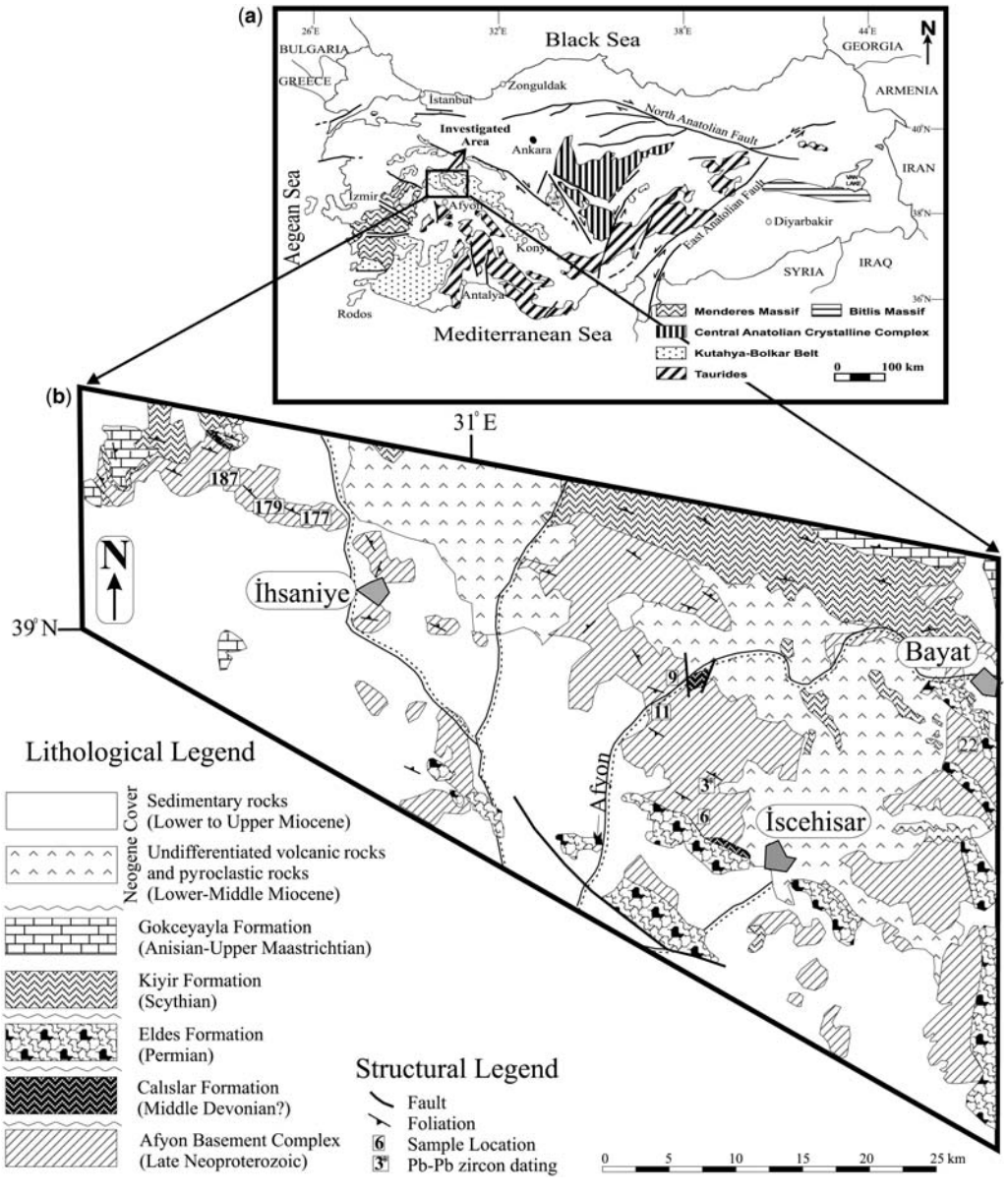

Fig. 1. (**a**) The main tectonic units of the Tauride–Anatolide Belt (modified after Goncuoglu *et al.* 1997); (**b**) geological map of NE Afyon (adapted from Özcan *et al.* 1989) showing exposures of Neoproterozoic to Upper Miocene rocks and location of samples that were collected for chemical and Pb–Pb analyses.

The Late Neoproterozoic low-grade metamorphic sediments and felsic igneous rocks in the Geyik Dag tectonic unit, slightly metamorphic rhyolites and granites, were described recently by Gürsu *et al.* (2004*a*) and Gürsu & Goncuoglu (2006). The Late Neoproterozoic basement rocks in the Kütahya–Bolkar Dagı tectonic unit, named the Afyon Basement Complex (ABC) (Gürsu *et al.* 2003), differ from the former by being mainly composed of quartz–albite–garnet–biotite schists intruded by porphyritic granites. The geochemical, tectonic and petrogenetic significance of

these granitic rocks is not well known and has not been previously studied. Hence, the nature of this Late Neoproterozoic basement and the tectono-magmatic framework of the felsic rocks within the Gondwanan evolution are unclear.

This paper presents new mineralogical, geochemical and geochronological data for Late Neoproterozoic porphyritic granitic rocks in the Kütahya–Bolkar Dagı unit, with the aim of interpreting their petrology, petrogenesis and tectonic significance. We then address possible correlations with the geochemical characteristics of the better-known felsic intrusions in the Geyik Dag tectonic unit, which is established as a representative of the Cadomian granitic magmatism in Peri-Gondwana.

Geological setting and petrography

The Afyon Basement Complex (ABC) as well as its Palaeozoic–Mesozoic cover in the Kütahya–Bolkar Dagı tectonic unit to the NE of Afyon has different stratigraphical and metamorphic features from that in the Sandikli area of the Geyik Dag unit.

In the area between Iscehisar–Bayat and Ihsaniye (Fig. 1) the ABC is mainly composed of quartz–albite–garnet–biotite schists, together with metamorphic porphyritic granitoids and micro-gabbroic stocks (Fig. 2). It is affected by extensive polyphase deformation and metamorphism and disconformably overlain by metaconglomerates and chlorite–quartz-schists alternating with laminated quartzites (Calıslar Formation of Gürsu *et al.* 2003, 2004*b*). The formation resembles the Devonian successions in the Taurides and is unconformably overlain by the Permian Eldes Formation (Goncuoglu *et al.* 1992, 2003). The metaconglomerates of the Eldes formation include pebbles of quartz-schist, mica-schists and metagranitic rocks, and the sequence continues upwards with quartzites, calc-schists and fossiliferous recrystallized limestones (Fig. 2). Here, the almost 2 km thick Early Cambrian–Late Ordovician units of the Geyik Dag unit are missing. The Mesozoic cover starts with Lower Triassic clastic deposits, followed by a continuous platform-type carbonate deposition that lasted without a depositional break until the Cretaceous. The entire succession has been affected by HP–LT Alpine metamorphism (Özcan *et al.* 1989; Goncuoglu *et al.* 1992; Candan *et al.* 2003, 2005), which has partly obliterated the metamorphic mineral parageneses of the earlier metamorphisms.

The country rocks of the ABC consist of metasedimentary rocks that are mainly composed of quartzo-feldspathic schists and garnet–mica schists (Gürsu *et al.* 2003) containing the assemblage quartz + albite + chlorite + white mica ± garnet ± biotite. In the northern part of Afyon, the granitic dykes are more abundant than elsewhere. The vertical to subvertical dykes vary in length (from 50 m to 10 km) and in width (from 50 cm to 25 m). $^{207}Pb-^{206}Pb$ zircon ages around 542 Ma from the intruding granitic rocks (in this study) indicate that the metasedimentary rocks are Precambrian in age. Based on the field observations and crosscutting relations (Fig. 3) the metabasic dykes represent younger intrusive events (Fig. 3a and b). They are micro-gabbroic dykes with the paragenesis albite ± sodic amphibole ± zoisite/epidote ± garnet (Candan *et al.* 2005) (Fig. 3a and b). On outcrops near NE Afyon, the metapelites, granitic rocks and metabasic dykes were affected by low-grade metamorphism prior to the Alpine HP–LT event (Goncuoglu *et al.* 2003; Candan *et al.* 2003, 2005). They show well-developed metamorphic foliations and multiphase deformations, ascribed to the Cadomian, Late Variscan and Alpine events (e.g. Gürsu *et al.* 2003, 2004*b*; Candan *et al.* 2005).

The felsic rocks in the study area are characterized by metamorphosed porphyritic granitoids and show evidence of multi-phase deformation. They mainly include relict igneous minerals such as alkali feldspar (disordered orthoclase) and sodic plagioclase (oligoclase–andesine in composition) (Fig. 4a). Biotite is the predominant ferromagnesian mineral in the granitoids. Highly fractured orthoclase and plagioclase crystals are observed in thin sections (Fig. 4a). Syntectonic albite porphyroblasts with linear muscovite inclusions (Fig. 4b) that grew synchronously with the early stages of crenulation cleavage are sharply discordant with external schistosity formed during a later deformational phase (Fig. 4b). Recrystallized quartz + fine-grained white micas (Fig. 4) grew synchronously with deformation under the low-grade metamorphic conditions during the Cadomian orogeny (Gürsu *et al.* 2003). As a result of metamorphic overprinting, the original microstructures and textures in the granitic rocks were ultimately lost and fine- to coarse-grained metamorphic quartz and white mica neo-formations developed. Mafic minerals such as biotite are rarely preserved, and were converted to chlorite during retrograde metamorphism. Accessory phases are mainly composed of titanite, zircon, monazite, apatite and rarely opaque minerals. A discrete crenulation cleavage is well developed in granitic rocks, with an S_1 fabric parallel to the main regional NNW–SSE foliation trend, overprinted by an S_2 cleavage at nearly 90° to S_1. S_3 has overprinted and folded the S_2 fabric diagonally at a low angle (30°) and may have developed during the Alpine event (Fig. 4c).

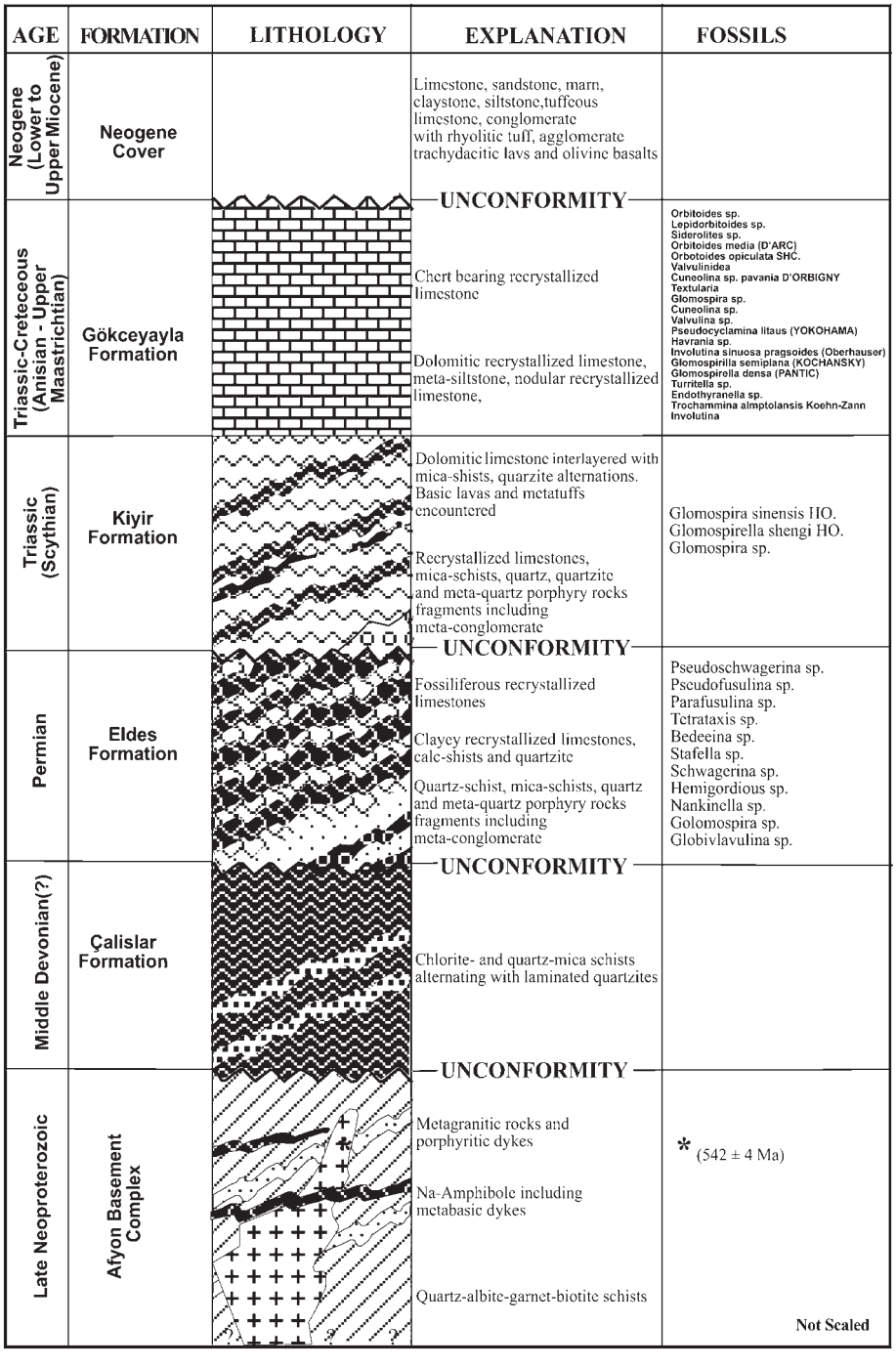

Fig. 2. Generalized columnar section of the NE Afyon area (after Gürsu *et al.* 2003, 2004*b*).

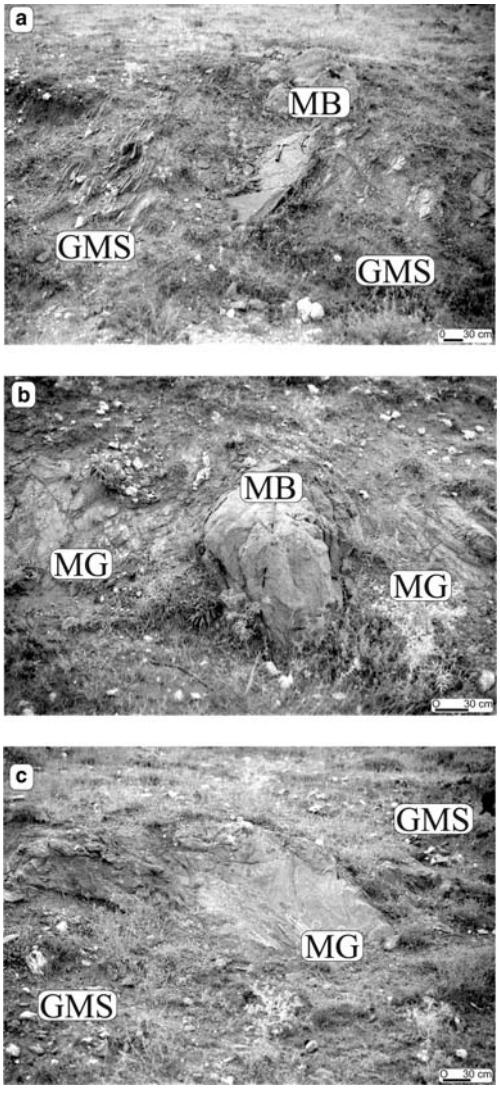

Fig. 3. Field occurrences of the intrusive rocks in the ABC: (**a**) and (**b**) metabasic dykes (MB) crosscut both garnet–mica schists (GMS) and granitic rocks (MG) of the study area; (**c**) the metamorphosed granitic rocks intrude the garnet–mica schists and show the development of metamorphic foliations and multiphase deformations.

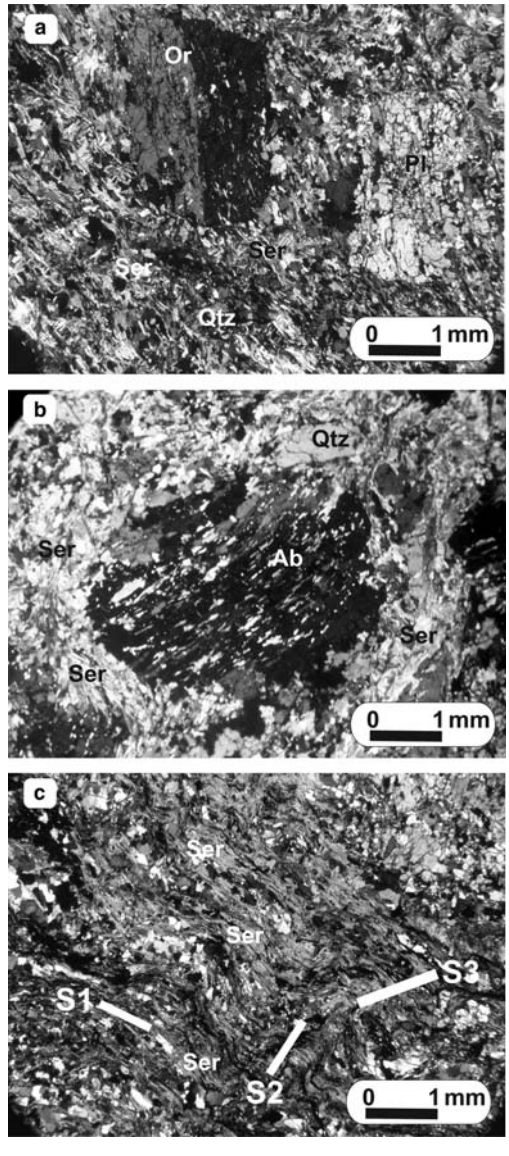

Fig. 4. (**a**) Microphotograph of the granitic rocks of the ABC. The highly fractured orthoclase (Or) and plagioclase (Pl) porphyroclasts are surrounded by very fine-grained recrystallized quartz (Qtz) and neoformation of sericite (Ser) parallel to mylonitic fabric. (**b**) Syntectonic albite (Ab) porphyroblasts with linear inclusion fabrics that are mainly composed of fine-grained white mica occurrence (Ser) and are sharply discordant with external schistosity. (**c**) Deformation and development of S_1, S_2 and S_3 planes in the granitic rocks of the ABC.

Analytical methods

Eight representative samples were analysed for major, trace and rare earth element (REE) abundances in Acme Laboratories, Vancouver, Canada. Determination of major element concentrations in rock samples expressed as common oxides for each element (SiO_2, TiO_2, Al_2O_3, Fe_2O_3, MnO, MgO, CaO, Na_2O, K_2O, P_2O_5 and Cr_2O_3), loss on ignition (LOI) and Sc were analysed by inductively coupled plasma atomic emission spectrometry

(ICP-AES) after fusion with lithium metaborate. The LOI was determined by weight difference after ignition at 1000 °C. Trace elements and REE were determined by inductively coupled plasma mass spectrometry (ICP-MS) following a lithium metaborate fusion and nitric acid digestion of 0.2 g samples. Analytical errors, as calculated from replicate analyses, are 0.5–1.0% for major elements and 0.5–3.5% for trace elements and REE.

Radiometric age dating is based on the single-grain zircon evaporation technique. The laboratory procedures were as described by Kober (1986). Zircons were separated by using a Wilfley table, magnetic separator, heavy liquids and finally hand-picking. Isotopic measurements on the typical magmatic igneous zircons were analysed by the $^{207}Pb-^{206}Pb$ evaporation technique on a Finnigan MAT 262 mass spectrometer at the University of Tübingen.

Single zircon Pb–Pb ages

Our new data for the Kütahya–Bolkar Dagı unit provide zircon ages for the granitic rocks. The calculated ages with the mean errors (2σ) for a sample from the Late Neoproterozoic basement analysed using the single zircon evaporation method are presented in Table 1. The $^{207}Pb-^{206}Pb$ ages determined by this method are considered to be minimum ages. Sample 3 is a light grey granitic rock from Doganlar near Iscehisar (see Fig. 1). The zircons are clear, transparent, euhedral and long-prismatic with some inherited cores. Based on Pupin's (1980) classifications, S_{17}, S_{18} and S_{19} pyramidal terminations were the predominant zircon crystal types in the granitic rocks. Five grains were evaporated and all produced different $^{207}Pb-^{206}Pb$ ages ranging from 541 ± 4 Ma to 2086 ± 4 Ma (Table 1; Fig. 5a and b). The cathodoluminescence (CL) images of zircon crystals in the granitic rocks commonly have magmatic domains representing zircons from the protolith (Fig. 5c and d). Additionally, some inherited cores, and some alteration features such as flow domains, recrystallization and the zigzag-shaped sector zoning on small rounded cores are also observed (Fig. 5d). Although this type of sector zoning is typical for metapelitic rocks, it has reported been also from metaigneous rocks (e.g. Vavra *et al.* 1996). Two grains (Grains 1 and 2) yielded $^{207}Pb-^{206}Pb$ ages of 541 ± 4 Ma and 542 ± 5 Ma with a mean of 542 ± 5 Ma (Fig. 5a). We are inclined to consider the two youngest grains as reflecting the time of emplacement of the granitic protoliths, and the ages are similar to those of the quartz porphyry rocks (543 ± 7 Ma, Kröner & Sengör 1990; 541.3 ± 10.9 Ma, Gürsu & Goncuoglu 2006) in the Sandikli area of the Geyik Dag unit. Additionally, similar ages have been obtained on the augen gneisses from the Menderes Massif ($^{207}Pb-^{206}Pb$ single zircon, 540–572 Ma, e.g. Hetzel & Reischmann 1996; Loos & Reischmann 1999; Koralay *et al.* 2004). The remaining three grains (Grains 3, 4 and 5) having brown, reddish, semi-transparent and well-rounded terminations provided xenocryst ages of 867 ± 5 Ma, 2062 ± 3 Ma and 2086 ± 4 Ma, respectively (Table 1; Fig. 5b). Three samples fall in the interval between 541 and 867 Ma with a peak at 542 Ma, whereas the oldest zircons show Palaeoproterozoic ages of 2.06–2.08 Ga. The peak zircon age (542 Ma) correlates with that of the post-tectonic intrusions that followed the Cadomian arc-related magmatism in northern Anatolia, which is dated at 565–590 Ma in NW Anatolia as well as along

Table 1. *Zircon morphology and Pb isotopic data from single grain evaporation*

Zircon morphology	Grain	Mass scans*	Evaporation temperature (°C)	$^{207}Pb-^{206}Pb$ ratio and 2σ error†	$^{207}Pb-^{206}Pb$ age and 2σ error
C, E, LP, T	1	190	1380	0.058301 ± 19	541 ± 4
C, E, LP, T	2	184	1400	0.058319 ± 24	542 ± 5
	1, 2‡	377		0.05831 ± 21.5	542 ± 5
C, E, LP, T	3	183	1380	0.067953 ± 26	867 ± 5
B, ST, WR	4	190	1400	0.127384 ± 11.8	2062 ± 3
R, ST, WR	5	106	1420	0.129081 ± 20.5	2086 ± 4

(Sample 3, porphyritic metagranite) B, brown; C, colourless; E, euhedral; LP, long prismatic; R, reddish; SR, sub-rounded; ST, semi-transparent; T, transparent; WR, well-rounded.
*Number of $^{207}Pb-^{206}Pb$ ratios evaluated for age assessment.
†Observed mean ratio corrected for non-radiogenic Pb where necessary. Standard errors based on uncertainties in counting statistics.
‡Mean ages calculated for two grains.

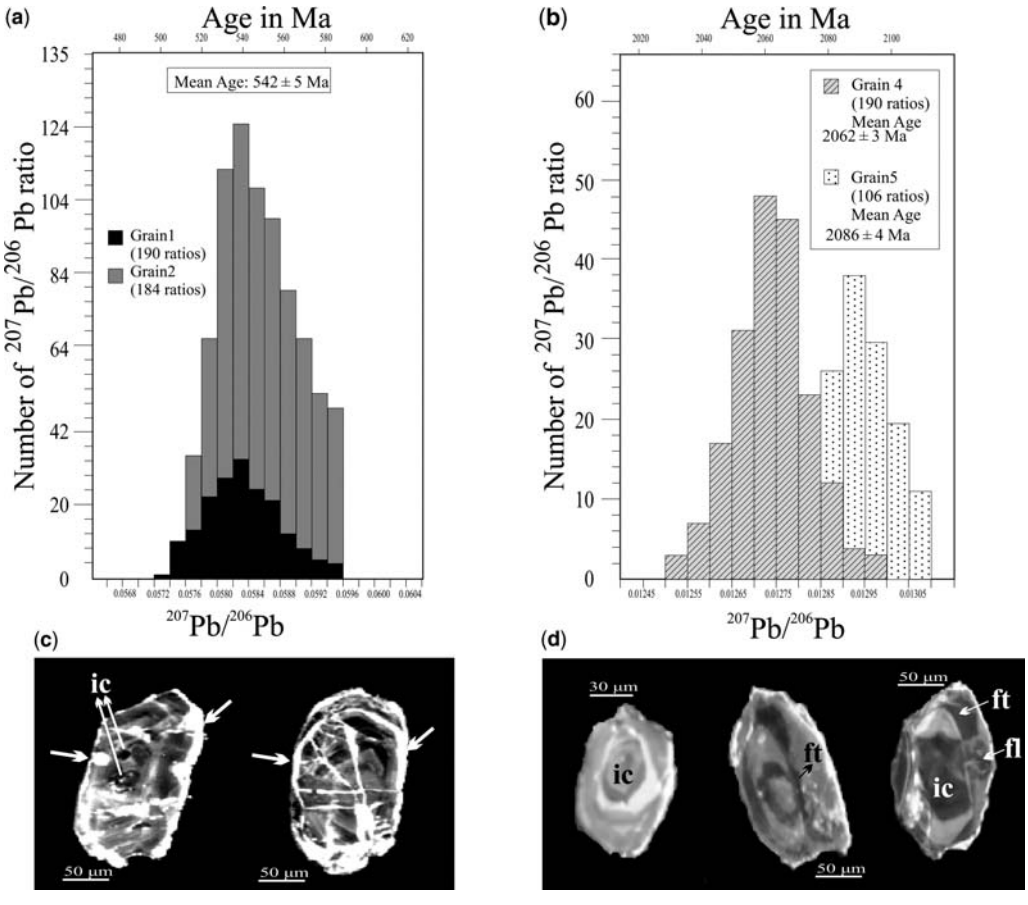

Fig. 5. Histograms showing distribution of radiogenic lead isotope ratios derived from evaporation of zircon populations obtained from the granitic rocks of the ABC. (**a**) Graph for two grains, integrated from 374 ratios and interpreted to reflect age of protolith emplacement. (**b**) Graph for xenocrystic grains of granitic rocks. (**c**) CL images show single-phase magmatic zoning with small resorbed and recrystallized areas; arrows indicate regions of oscillatory zoning. (**d**) CL images showing typical internal structures. ic, rounded inherited cores; fl, flow domains; ft, sector zoning.

the northern margin of the Peri-Gondwana (e.g. Chen *et al.* 2002; Gürsu & Goncuoglu 2005; Ustaömer *et al.* 2005). Arc-related magmatism and post-tectonic granitoid emplacement have also been observed in many Cadomian basements in Armorica and NW France (540–746 Ma, Egal *et al.* 1996; Strachan *et al.* 1996; Ballèvre *et al.* 2001; Chantraine *et al.* 2001), Saxo-Thuringia, northern Germany (540–660 Ma; Linnemann *et al.* 2000; Linnemann & Romer 2002; Mingram *et al.* 2004), the Iberian massif, southern Spain (540 to 575–600 Ma, e.g. Bandres *et al.* 2002; Pin *et al.* 2002), Tepla–Barrandia (Bohemia), Czech Republic (550–670 Ma, Dörr *et al.* 2002; Linnemann & Romer 2002; Patočka & Štorch 2004) and the Carpathians, Romania (567–777 Ma, Liégeois *et al.* 1996). The older ages obtained in this study are generally from brown–reddish, sub-rounded to well-rounded zircon grains that are interpreted as xenocrysts from the chronologically heterogeneous Palaeoproterozoic basement. These older zircon ages (2.06–2.08 Ga) have been documented from the Eburnean basement of the West African craton (Allègre & Ben Othman 1980; Egal *et al.* 2002; Hirdes & Davis 2002; Linnemann *et al.* 2004; Murphy *et al.* 2004). The data presented here also support the conclusions of Goncuoglu *et al.* (1997) and Gürsu & Goncuoglu (2006) that Tauride–Anatolite Platform was derived from the NW margin of Gondwana during the Late Neoproterozoic–Early Palaeozoic.

Geochemistry

Major and trace element and REE element concentration of granitic rocks in the ABC are listed in Table 2. The rocks span a wide range of SiO_2 contents (66.31–73.68 wt%), are of subalkaline affinity and plot in the rhyodacite–dacite field on the Zr/TiO_2–Nb/Y discrimination diagram of Winchester & Floyd (1977) (Fig. 6a). High-silica rocks are subdivided into peralkaline, peraluminous and meta-aluminous groups on the basis of the alkali index (Hildreth 1981; Leat *et al.* 1986; Davies & MacDonald 1987; Kirstein *et al.* 2000). The granitic rocks show evidence of alkali mobility, which may affect the classification based on alkali elements. To avoid any misinterpretations for alkali indices, Nb–Zr variation diagrams (Leat *et al.* 1986) were used to determine the geochemical signatures of the granitic rocks. The log–log Nb v. Zr diagram shows a very scattered positive trend with $<$326 ppm Zr and $<$14 ppm Nb and the data plot close to the subalkaline fiew, characteristic of peraluminous magmas (Fig. 6b). Major element variations for the granitic rocks in the NE Afyon area are shown on selected Harker diagrams (Fig. 7). Al_2O_3 (11.57–15.56 wt%), Fe_2O_3 (3.71–5.58 wt%), K_2O (1.70–3.99 wt%), MgO (1.79–2.51 wt%) and TiO_2 (0.64–0.82 wt%) concentrations decrease with increasing SiO_2 contents defining a nearly linear trend, and suggest that these rocks are probably products of magmatic differentiation from a parental magma (Fig. 7). K_2O (1.70–3.99 wt%) decreases along a hyperbolic curve, reaching near-one concentrations with increasing SiO_2, which shows that the major part of the granitic rocks is high- to medium-K calc-alkaline. CaO (0.22–1.23 wt%) and Na_2O (1.12–3.10 wt%) contents correlated very poorly with SiO_2 as a result of the element mobility during the metamorphism (Fig. 7).

The total alkali concentrations ($Na_2O + K_2O$) in granitic rocks are uniform but have low values (4.13–6.06 wt%). The higher LOI (2.9–3.22 wt%), lower to high K_2O/Na_2O ratios (0.60–3.56), Na_2O–SiO_2, CaO–SiO_2 and Sr–SiO_2 variations indicate that the felsic rocks have been affected by alkali mobility related to the low-grade metamorphism and albitization. Consideration of major elements such as Na and K, which are commonly influenced by albitization, substantiates the outcome of the Na-metasomatism in the granitic rocks. This is in support of petrographical observations that potassium feldspar is affected by albitization, but relatively low Na_2O/K_2O ratios also indicate that some of original potassium feldspar is still preserved in the granitic rocks. Rb depletion also may have been a likely consequence of chloritization and argillitic alteration (breakdown of feldspar and mica). Sample 22 has abnormally high silica content (73.68 wt%) and may reflect the locally silicification related to the secondary process (Fig. 7). Hence, SiO_2, alkalis, Rb and Sr are not used in further geochemical diagrams to avoid any misinterpretation resulting from secondary processes.

Variations of trace elements against SiO_2 are plotted in Figure 7. Ba (316–823 ppm), Rb (68–140.9 ppm), Nb (9.3–14.3 ppm), Th (9.3–16 ppm), V (69–105 ppm), Zr (181.8–326.5 ppm), Ce (46.7–91.1 ppm), Y (19.9–30.7 ppm) and Lu (0.3–0.49 ppm) show well-defined negative trends with increasing SiO_2 (with the exception of Sr (29.4–84.3 ppm)), indicating the fractionation of plagioclase, alkali feldspar, biotite, titanite, zircon and iron oxides, respectively (Fig. 7). The relatively high values for large ion lithophile elements (LILE) and high field strength elements (HFSE) such as Nb (average 11.8 ppm), Rb (average 95 ppm), Y (average 26), Ce (average 67 ppm), Zr (average 251 ppm), Ta (0.8 ppm), and Yb (average 2.5 ppm), and the ratios Ti/Zr (15.5–22.5 ppm), Ti/Y (135.5–216.8 ppm), Nb/Y (0.33–0.55 ppm) and Zr/Nb (16.5–28.3 ppm) in the granitic rocks are relatively consistent with average chemical composition of the Proterozoic tonalite–trondhjemite–granodiorite (TTG: 7.1, 63, 17.3, 45, 152, 0.72, 1.33, 18.5, 162.8, 0.41 and 21.4, respectively) (average data taken from Condie 2005).

Chondrite-normalized (Sun & McDonough 1989) trace elements patterns of the granitic rocks are characterized by slightly enrichment in Ba, Th, La, Ce, Nd and Zr with depletion of Rb, K, Nb, Sr, P and Ti (Fig. 8a). The distinct Rb and Sr anomaly may also be ascribed to mobilization during the metamorphism. Chondrite-normalized REE patterns of granitic rocks show light REE (LREE) enrichment with respect to heavy REE (HREE), and negative Eu anomalies are moderately pronounced, with Eu/Eu* between 0.61 and 0.71 (Fig. 8a). The negative Eu anomaly in the chondrite-normalized REE plot suggests that plagioclase and alkali feldspar fractionation within the stability field of feldspar has played a significant role in formation of these granitic rocks and indicates intracrustal fractionation. The granitic rocks have moderate to high REE contents ($\sum$ REE 99.8–196.8 ppm) with fractionated $(La/Yb)_N = 4.6–10$ and $(La/Sm)_N = 2.6–3.7$, and relatively flat $(Gd/Yb)_N = 1.02–1.85$. The LILE and REE chondrite-normalized patterns display very similar patterns to the average chemical composition of Proterozoic TTG (Fig. 8b).

The continuous negative trends of granitic rocks in Nb/U–U and Ce/Pb–Pb variations indicate that U and Pb may have been added as a result of intracrustal melting (Fig. 8c and d), and the low Nb/U ($<$10) and variable Ce/Pb ($<$65) ratios

Table 2. *Representative chemical analyses of granitic rocks in the ABC to the NE of Afyon in the Kütahya–Bolkar Dagı unit*

Sample no.	Afyon3	Afyon6	Afyon9	Afyon11	Afyon22	Afyon177	Afyon179	Afyon187	Average
SiO_2	68.52	66.87	70.29	68.61	73.68	67.90	69.11	66.31	68.91
TiO_2	0.69	0.65	0.72	0.82	0.64	0.69	0.77	0.81	0.72
Al_2O_3	14.49	15.55	13.71	13.74	11.57	14.48	13.67	15.56	14.09
Fe_2O_3	4.99	5.58	4.56	5.56	3.71	4.46	5.35	5.57	4.97
MnO	0.05	0.05	0.05	0.08	0.04	0.04	0.09	0.08	0.06
MgO	2.21	1.80	1.79	2.51	1.81	2.15	2.0	2.47	2.09
CaO	0.53	0.22	0.44	0.60	0.36	1.23	0.39	0.41	0.52
Na_2O	1.12	2.68	2.97	2.10	2.38	3.09	2.81	3.10	2.28
K_2O	3.99	3.38	2.01	2.70	1.75	2.54	1.70	2.45	2.56
P_2O_5	0.21	0.18	0.23	0.20	0.24	0.24	0.21	0.22	0.21
Cr_2O_3	0.019	0.009	0.015	0.014	0.014	0.011	0.012	0.013	0.013
LOI	3.1	3.2	3.0	2.9	3.8	3.1	3.6	3.1	3.2
Total	100.02	100.25	99.84	99.93	100.04	100.01	99.77	100.17	100.00
Ba	823	688	420	728	316	658	483	622	592
Sc	13	19	12	12	9	12	12	14	13
Co	13	8.4	9.4	13.4	9.8	11.4	14.9	12.6	11.6
Pb	10	14.8	4	1.4	13.8	4.5	2.2	22.3	9.1
Zn	70	67	61	80	85	56	75	86	72
Ni	52.5	18.5	31.2	43.2	32.4	27.6	36.9	38.3	35.1
Cs	4	2.4	2.4	4	2.7	3.1	2.7	2.6	3.0
Ga	20.7	21.4	16.8	18.2	14.4	18	17.4	20.1	18.4
Hf	6.2	7.4	6.7	9.7	7.9	7.4	7.6	6.2	7.4
Nb	11.6	12.2	11	14.3	9.3	11.1	11.9	13.1	11.8
Rb	140.7	120.3	81.7	99.6	68	87.8	68.7	89.7	94.6
Sr	80.9	33.2	84.3	58.7	41.7	29.4	63.6	49.9	55.2
Ta	0.80	0.80	0.80	0.90	0.7	0.8	0.8	1.0	0.8
Th	12.4	12.1	11.7	16	9.3	12.2	10.4	11.2	11.9
U	2.4	1.4	1.9	3.0	2.1	2.3	1.7	1.8	2.1
V	98	105	93	94	69	89	93	97	92
W	1.7	1.2	0.6	1.2	1.0	0.8	1.7	1.1	1.2
Zr	191.8	251.6	246	326.5	263	231	279.4	216.1	250.6
Y	21.2	27.4	19.9	25	28.3	28.4	30.2	30.7	26.4
La	15.9	18.3	20.9	38.6	32.3	31.1	29.7	37.1	28.0
Ce	46.7	62.1	56.6	91.1	61.0	76.9	61.8	75.9	66.5
Pr	3.72	4.05	4.75	7.87	6.60	6.74	6.22	7.72	5.95
Nd	16	17.8	19.1	33.8	27.2	28	25.8	31.8	24.9
Sm	3.8	3.8	3.9	6.6	5.7	5.8	5.3	6.6	5.2
Eu	0.78	0.76	0.80	1.20	1.39	1.30	1.17	1.40	1.10
Gd	3.26	3.37	3.22	5.38	5.63	5.71	5.31	5.57	4.68
Tb	0.64	0.63	0.53	0.86	0.92	0.89	0.82	0.86	0.76
Dy	3.30	4.18	2.81	4.53	4.74	4.91	4.76	5.0	4.27
Ho	0.66	0.87	0.56	0.83	0.89	0.86	0.92	0.89	0.81
Er	2.24	2.76	1.94	2.67	2.86	2.95	2.97	2.95	2.66
Tm	0.28	0.35	0.22	0.35	0.31	0.41	0.40	0.38	0.33
Yb	2.21	2.69	1.84	2.61	2.47	2.71	2.68	2.89	2.51
Lu	0.36	0.44	0.30	0.44	0.38	0.43	0.46	0.49	0.41
Ti	4135	3896	4315	4915	3836	4135	4615	4855	4338
Zr/Y	9.04	9.18	12.36	13.06	9.29	8.13	9.25	7.04	9.66
Th/Nb	1.07	0.99	1.06	1.12	1.00	1.09	0.87	0.85	1.00
Th/Y	0.58	0.44	0.58	0.64	0.33	0.43	0.34	0.36	0.46
Y/Nb	1.82	2.24	1.81	1.74	3.04	2.56	2.53	2.34	2.26
La/Nb	1.37	1.50	1.90	2.69	3.47	2.80	2.49	2.83	2.38
Ti/Y	195.08	142.2	216.8	196.6	135.55	145.6	152.8	158.1	167.8
$(La/Yb)_N$	4.86	4.60	7.68	9.99	8.84	7.75	7.49	8.67	7.48
$(La/Sm)_N$	2.63	3.03	3.37	3.68	3.57	3.38	3.53	3.54	3.34
$(Gd/Yb)_N$	1.20	1.02	1.42	1.67	1.85	1.71	1.61	1.56	1.50
Eu/Eu*	0.68	0.65	0.71	0.61	0.75	0.69	0.67	0.70	0.68

Subscript N indicates normalization data from Sun & McDonough (1989).

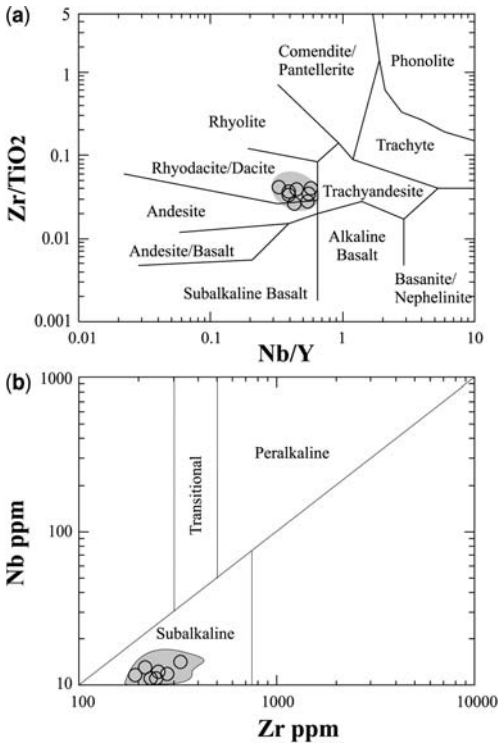

Fig. 6. (**a**) Zr/TiO_2 v. Nb/Y diagram (Winchester & Floyd 1977) and (**b**) Nb–Zr diagram (Leat *et al.* 1986) for granitic rocks of the ABC; O, granitic rocks.

suggest magmatic differentiations of intracrustal melting of a TTG source that is in the garnet stability field under the mantle wedge (Martin *et al.* 2005; Condie 2005). The low to very low unfractionated HREE and Y abundances suggest that the granitic rocks were evolved from second-stage melts of a TTG source during intracrustal melting without residual garnet.

To summarize, the geochemical variations confirm that the granitic rocks are sub-alkaline (peraluminous) in composition. They have geochemical characteristics of I-type (TTG source) felsic intrusive rocks and magmatic differentiations such as fractional crystallization trends are observed in geochemical diagrams. Trace element and REE patterns show similar patterns, with distinctive depletion in Rb, K, Nb, Sr, P and Ti relative to the other trace elements. Trace element and REE patterns correlate very well with the Proterozoic TTG data.

Magmatic temperatures, crystallization and source rock conditions

In this study, emplacement temperatures were estimated by using zircon, monazite and apatite saturation thermometry (Table 3). Petrographic and geochemical signatures of the granitic rocks from the study area show that the felsic magmas must have been saturated in zircon, monazite and apatite minerals. Zircon, monazite and apatite saturation temperatures can be calculated from whole-rock geochemical data to estimate temperatures and composition effects of crustal magma types by using the experimental models of Watson & Harrison (1983), Harrison & Watson (1984), Montel (1993) and Piccoli *et al.* (1999). Hydrothermal experiments in the temperature range of 750–1020 °C show the saturation behaviour of zircon in crustal anatectic melts as a function of both temperature and the zircon solubility range in peraluminous granites changing from *c.* 100 ppm dissolved at 750 °C *c.* 1330 ppm at 1020 °C (Watson & Harrison 1983). The zircon solubility model of Watson & Harrison (1983) is given by equation

$$\ln D_{Zr} = \{-3.80 - [0.85 \times (M-1)]\} + 12900/T$$

where T is zircon saturation temperature (in °C), D_{Zr} is the bulk concentration of Zr and M is the cationic ratio $[(Na + K + 2 \times Ca)/(Al \times Si)]$ of the whole-rock concentration of SiO_2, Al_2O_3, NaO, K_2O, CaO. The Zr concentration and cationic ratio (M) show similar scatter in granitic rocks (192–327 ppm; 0.70–1.05). Zircon saturation temperatures of granitic rocks have a distinct peak at 790–809 °C with only one higher value at 820 °C (average 803 °C) (Table 3).

Harrison & Watson (1984) showed that the whole-rock concentrations of SiO_2 and P_2O_5 of granitic rocks were equivalent to the initial melt composition of apatite crystallized from the melt. Apatite precipitation in peralkaline, meta-aluminous, slightly peraluminous and highly peraluminous silicate melts (excluding low-Ca melts) can be approximated as a function of P_2O_5 and SiO_2 (Harrison & Watson 1984; Pichavant *et al.* 1992). Apatite saturation temperatures at the temperature at which apatite began to crystallize from the magmas were calculated by using SiO_2 and P_2O_5 in the following equation of Piccoli *et al.* (1999), which is adapted from Harrison & Watson (1984):

$$T = (26400 \times C^1SiO_2 - 4800)/ (12.4 \times C^1SiO_2 - \ln(C^1P_2O_5) - 3.97) - 273.15$$

where T is the apatite saturation temperature (in °C), and C^1SiO_2 and $C^1P_2O_5$ are the concentration of silica and phosphorus (expressed as weight fractions in the melt at the apatite

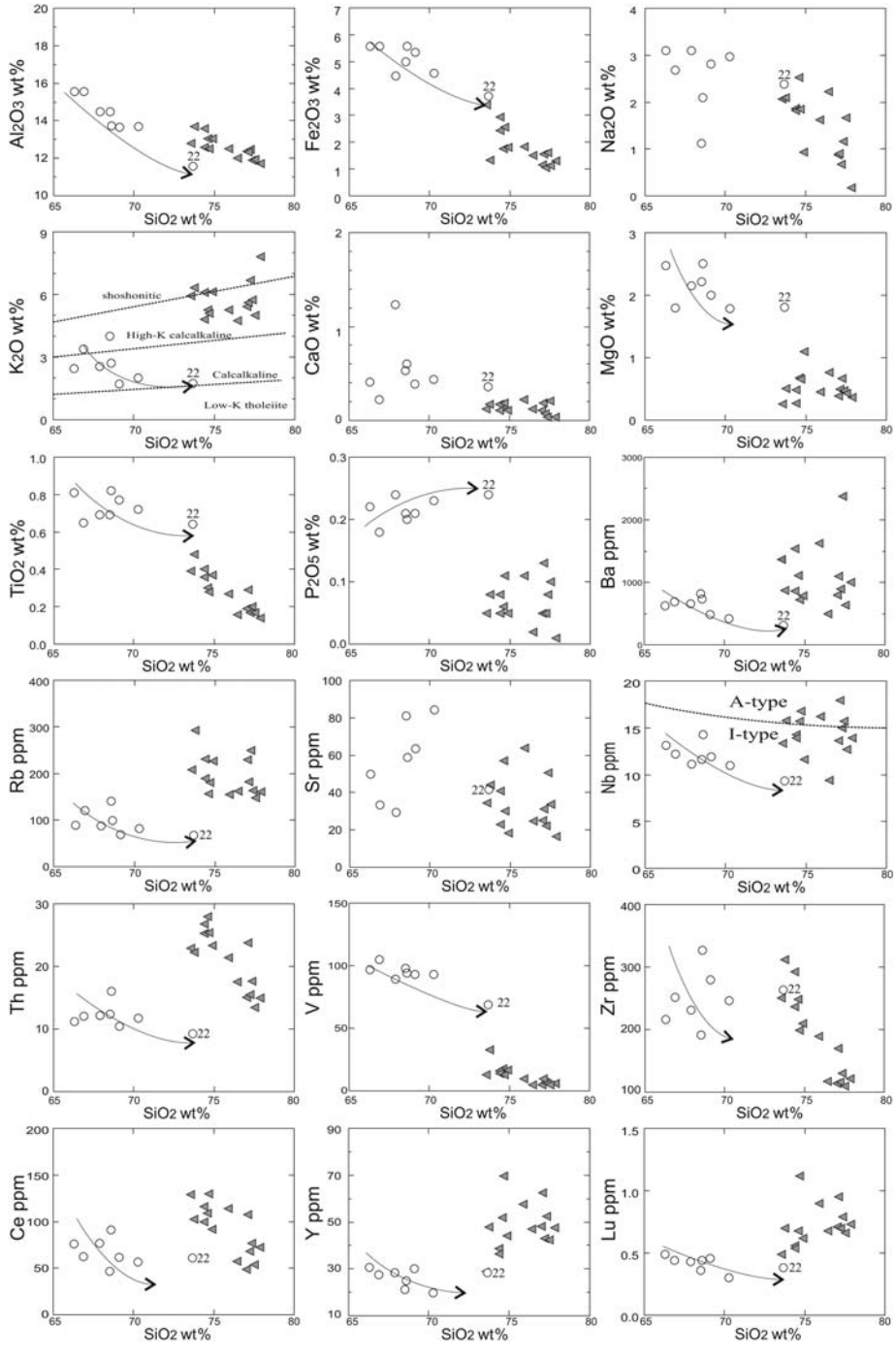

Fig. 7. Major and selected trace element variation diagrams v. SiO_2 (field boundaries for K_2O, I- and A-type granites are from Peccerillo & Taylor (1976) and Collins *et al.* (1982), respectively); ○, granitic rocks; ◄, quartz porphyry rocks of Geyik Dag Unit in Sandikli, SW Afyon (data taken from Gürsu & Goncuoglu 2006).

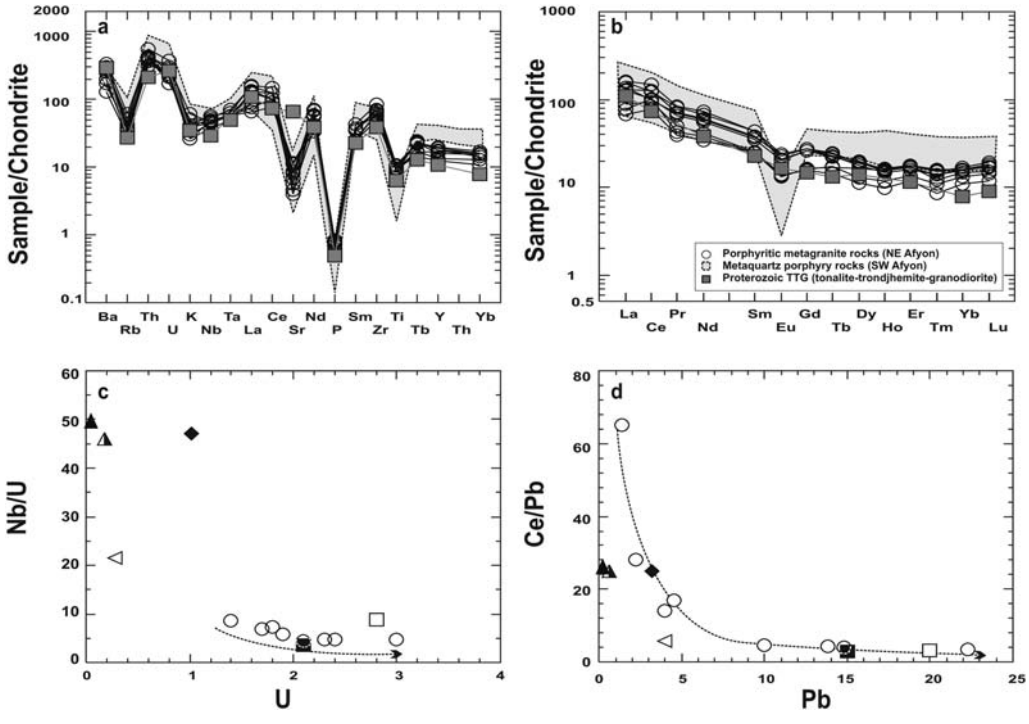

Fig. 8. (**a**) Chondrite-normalized trace multi-element diagram; (**b**) chondrite-normalized REE patterns (all normalizing values from Sun & McDonough 1989). Shaded area for quartz porphyry rocks is from Gürsu & Goncuoglu (2006). (**c**) and (**d**) Nb/U–U and Ce/Pb–Pb diagrams. O, granitic rocks; □, upper crust; ◁, lower crust; ▲, N-MORB (mid-ocean ridge basalt); half-filled triangles, enriched mid-ocean ridge basalt (E-MORB); ◆, ocean-island basalt (OIB); ■, TTG. Upper and lower continental crust, N-MORB, E-MORB, OIB and TTG data are from Taylor & McLennnan (1995), Sun & McDonough (1989) and Condie (2005), respectively.

crystallization temperature). Piccoli & Candela (1994) and Piccoli *et al.* (1999) showed that the relationship between the SiO_2 and P_2O_5 bulk concentrations in the initial melt can be used for the apatite crystallization temperature at crustal pressures. This equation is based on the kinetic studies on the solubility of apatite in felsic melts by Harrison & Watson (1984), and is valid at crustal pressures for rocks with 45–75 wt% SiO_2 and $<10\%$ H_2O (Harrison & Watson 1984). The

Table 3. *The zircon, monazite and apatite saturation temperatures of granitic rocks in the ABC*

Sample no.	Zircon saturation temperature (°C)	Monazite saturation temperature (°C)	Apatite saturation temperature (°C)
Afyon3	820	833	970
Afyon6	802	836	935
Afyon9	803	830	998
Afyon11	790	886	965
Afyon22	804	860	1035
Afyon177	797	827	979
Afyon179	799	862	976
Afyon187	809	873	952
Average	803	851	976

average SiO_2 and P_2O_5 weight concentrations of granitic rocks are distinguished by being lower 64.5–73.4% (average 68.9%) and higher 0.18–0.24% (average 0.24%), respectively. The estimates of apatite saturation temperatures of granitic rocks have a distinct peak at 935–979 °C with only two higher values at 998–1035 °C (average 976 °C) (Table 3).

As shown by petrography, monazite is the main LREE-bearing mineral in less evolved granitic rocks. In contrast to zircon, the monazite solubility is strongly dependent on the H_2O contents in Ca-poor felsic magmas (Montel 1993) and is described in the following equation of Montel (1993):

$$\ln(\mathrm{REE_t}) = 9.50 + 2.34D + 0.3879\sqrt{H_2O} - 13318/T - 273.15$$

where $\mathrm{REE_t} = \sum$[REE (ppm)/atomic weight (g mol^{-1})], D is the cationic % $(\mathrm{Na + K + Li + 2Ca})/\mathrm{Al(Al + Si)}$, H_2O is in wt% and T is the monazite saturation temperature (in °C). The REE considered extend from La to Gd, excluding Eu (Montel 1993). We calculated temperatures for 3.5 wt% H_2O, which is a typical value expected in crustal magmas (Thomson 1996). Estimated monazite saturation temperatures of granitic rocks have a distinct peak at 827–836 °C with higher values at 860–886 °C (average 851 °C); (Table 3). The monazite saturation temperatures are compatible with zircon data rather than apatite data for the studied granitic rocks from the ABC. The calculated apatite saturation temperatures are higher than those obtained from the zircon and monazite saturation thermometry by 100–180 °C. To justify this discrepancy, Pichavant *et al.* (1992) noted that the calibration of Harrison & Watson (1984) fails to yield reliable results in peraluminous rocks, and all the granitic rock samples from the ABC contain low CaO (about <1.0 wt%). Additionally, Winchester & Floyd (1976) found that P could easily show mobility as a result of progressive alteration and metamorphism, and this may affect the apatite saturation thermometry. In a source rock without monazite, apatite dissolution will release both LREE and phosphorus into the melt and if REE in melt become oversaturated, monazite crystallization occur (Zeng *et al.* 2005). The mineralogical–petrographical analyses of the granitic rocks show that zircon and monazite crystallized early. They occur as small inclusions within the mica minerals with grain sizes of about 0.024–0.045 mm and 0.032–0.152 mm, respectively.

The Pb–Pb systematics of the zircon from the granitic rocks in the ABC indicates the presence of an inherited older crustal component, and inherited zircons were partly dissolved in the melt. The zircon temperatures may be suggestive of a high proportion of assimilated crustal material in the magmas. Therefore zircon saturation temperatures calculated from total Zr abundances may be higher than the real temperatures of magmas. We obtained slightly higher temperatures (790–820 °C) for the granitic rocks of the Neoproterozoic basement by using zircon thermometry. Our average estimates of zircon, monazite and apatite saturation temperatures in the felsic magmas range from 803 to 976 °C. The calculations provide a reasonable estimate of the temperatures over which zircon and monazite crystallized. On the other hand, based on Pupin's (1980) classifications, S_{17}, S_{18} and S_{19} pyramidal terminations (see Table 3) in the studied granitic rocks were the predominant zircon crystal types, indicating temperatures of 800 ± 50 °C. These results suggest that the felsic magma temperatures were between *c.* 800 °C and *c.* 850 °C in the studied granitic rocks of the ABC and could be interpreted as temperatures of LREE and Zr saturation at the onset of monazite and zircon crystallization.

The generation of I-type granite melts requires substantially higher temperatures (800–900 °C) than that of S-type granitoid melts ($\leq$700 °C), as shown by experimental work (e.g. Liew & McCulloch 1985). Estimated magma temperatures of the granitic rocks in this study of about 850 °C are in agreement with I-type rather than S-type granite melts. $Nb–SiO_2$ and $Y–SiO_2$ variation diagrams (see Fig. 7) also indicate an I-type source (Collins *et al.* 1982) rather than S- and A-type granitic rocks. In addition to these data, $Al_2O_3–SiO_2$ variations also identify the compositional differences of experimental melts produced by partial melting of various source rocks (Helz 1976; Spulber & Rutherford 1983; Beard & Lofgren 1989, 1991; Winther & Newton 1991; Wolf & Wyllie 1994). The protoliths of granitic rocks of the ABC are probably homogeneous and may have originated from crust-derived (probably TTG-like compositions with negative Eu and flat HREE) felsic magmas and may have been generated from a chemically similar magma source.

Magma modelling and the generation of felsic magmas

The decrease in Zr abundance with increasing SiO_2 suggests that zircon was a fractionating phase (e.g. Watson & Harrison 1983). The multi-element behaviour is characterized by lower

abundances of Rb, K, Nb, Sr, P and Ti and higher abundances of Ba, Th, La, Ce, Nd and Zr suggesting a source similar to TTG. The flat HREE patterns in the metagranitic rocks show that garnet was not restite phase, which indicates that the felsic magmas were formed at pressures <10 kbar (Rutter & Wyllie 1988; Vielzeuf & Montel 1992); this implies crustal depths of melting.

The granitic rocks have low silica (66.3–73.6 wt%) and relatively low to high alumina (11.5–15.5 wt%) contents consistent with partial melting of an igneous source (average 67.3 wt% SiO_2 and average 15.8 wt% Al_2O_3 in TTG; average 73.16 wt% SiO_2 and 13.90 wt% Al_2O_3 in granites; 73.12 wt% SiO_2 and 13.82 wt% Al_2O_3 in felsic volcanic rocks, respectively) rather than a sedimentary protolith (65.83 wt% SiO_2 and 15.33 wt% Al_2O_3 in greywackes; 63.50 wt% SiO_2 and 17.72 wt% Al_2O_3 in cratonic shales (e.g. Condie 1993, 2005; Chappell 1999). The trace element and REE pattern and variation diagrams (see Fig. 8) indicate that the source was igneous with Ti/Zr (average 20.97), Nb/Y (average 0.45), Zr/Nb (average 21.42), Th/Y (average 0.46) and La/Nb (average 2.38) ratios similar to those of TTG (18.5, 0.41, 21.4, 0.35 and 3.66, respectively; data from Condie (2005)). All these data support the idea that the granitic rocks in the ABC may be derived from dehydration melting of a TTG source rather than from sedimentary protolith. Experimental data also support that dehydration of tonalites may produce granitic melts within the temperature range 750–900 °C at 2–10 kbar pressure (Sing & Johannes 1996*a*, *b*), and peraluminous tonalites can contain up to about 30% biotite + muscovite and quartz + plagioclase concentrations, which suggests remelting to yield mobile granitic magmas (Patiño & Patiño-Douce 1987).

The TTG source composition (Condie 2005) was used as the possible source rock (C_0), and fractional melting and Rayleigh fractional crystallization process were modelled by using Rb, Ba, K, Sr, Nb, Th, U, Zr, Ti, Y, La, Ce, Nd, Sm, Eu, Gd, Tb, Dy, Er, Yb and Lu to constrain the generation of granitic rocks. The phase proportions were estimated from the normative mineralogy of possible source rocks and partition coefficient values (D_0) were calculated assuming 51% plagioclase, 21.5% quartz, 11.5% alkali feldspar, 11% amphibole and 5% biotite in the source residue with mineral–melt coefficient for dacitic–rhyolitic magma compositions (Arth 1976; Pearce & Norry 1979; Henderson 1982; Watson & Harrison 1983; Nash & Crecraft 1985; Table 4). The fractional melting and Rayleigh crystallization were used to determine the approximate minor and trace element, and REE compositions. Bulk D_0^1 values for the Rayleigh crystallization modelling were calculated from average normative mineralogical contents of granitic rocks considered as an assemblage of 43.7% quartz, 21.4% plagioclase, 15.7% alkali feldspar, 7.3% corundum, 5.4% orthopyroxene, 5.2% magnetite and 0.48% apatite. Calculated 20% fractional melting plus 20% fractional crystallization of TTG source rocks gives similar trends to those of granitic rocks (Table 5, Fig. 9a and b). Experimental data (e.g. Clemens & Vielzeuf 1987; Rutter & Wyllie 1988; Sing & Johannes 1996*a*, *b*) also show that melt proportions obtained by dehydration melting of tonalites may increase to nearly 15 vol% at 850 °C and 22.5 vol% at 900 °C; these values are similar to the 20% partial melting of a TTG source in our modelling study.

Chondrite-normalized calculated compatible/incompatible element patterns, shown in Figure 9a, are very similar to those of the studied granitic rocks and display enrichment in Ba, La, Ce, Nd, Zr and Y and depletion in Rb, K, Nb, Sr and Ti. Sr and Ti negative anomalies are consistent with significant fractional crystallization. The REE pattern of the calculated TTG melts also shows a pattern concordant with that of the granitic rocks and displays an enrichment of LREE rather than HREE and a pronounced negative Eu anomaly (Fig. 9b). A 20% fractional melting and 20% fractional crystallization of a Proterozoic TTG source provides a significant control on the change in Eu/Eu* with increasing Th abundances for the studied granitic rocks (Fig. 10).

In conclusion, we suggest that the felsic magmas in western Anatolia were generated by dehydration melting of a TTG source at <10 kbar pressure. Our petrogenetic modelling also implies that the granitic rocks were developed from partial melting of a TTG source by 20% fractional melting plus 20% Rayleigh fractional crystallization.

Comparison of the Neoproterozoic granitic magmatism in the basements of Kütahya–Bolkar Dagı and Geyik Dag tectonic units

The metaquartz porphyry rocks in the Geyik Dag unit in the Sandikli area display petrographical and chemical differences from the granitic rocks of the Kütahya–Bolkar Dagı unit in the NE Afyon area. The zircon and apatite thermometers of metaquartz porphyry rocks in Sandikli yielded two distinct peaks at 783–811 °C and 821–845 °C (average 816 °C) and three distinct peaks at 785–823, 881–925 and 947–998 °C (average 912 °C), respectively, and include well-developed perthitic textures (Table 6). The phenocryst phase

Table 4. *Mineral–melt partition coefficients for dacitic–rhyolitic melts used in the modelling of fractional melting and Rayleigh fractional crystallization*

Distribution coefficients	Quartz melt*	K-feldspar melt*	Plagioclase melt*	Biotite melt*	Hornblende melt†	Orthopyroxene melt*†	Apatite melt†	Magnetite melt†
Rb	0.041	1.75	0.105	3.20	0.014	0.003		
Ba	0.022	6.12	1.515	6.36	0.044	0.003		
Th	0.009	0.023	0.048	1.227		0.13		
U	0.025	0.048	0.093	0.167		0.145		
K	0.013	1.490	0.1	5.63	0.081	0.02		
Nb			0.06	6.367	4.0	0.8	0.1	
Sr		3.87	4.4	0.447	0.022	0.009		
Zr		0.03	0.135	1.197	4.0	0.2	0.1	0.8
Ti	0.038		0.05		7.0	0.4	0.1	12.5
Y			0.13	1.233	6.0	1.0	40	2.0
La	0.015	0.08	0.38	5.713		0.78	14.5	
Ce	0.014	0.037	0.267	4.357	1.52	0.93	34.7	
Nd	0.016	0.035	0.203	2.56	4.26	1.25	57.1	
Sm	0.014	0.025	0.165	2.117	7.77	1.6	62.8	
Eu	0.056	4.45	1.214*	0.87*	5.14	0.825	30.4	
Gd			0.125	0.067	10.0	0.34	56.3	
Tb	0.017	0.025		1.957		1.85		
Dy	0.015	0.055	0.112	1.72	13.0	1.8	50.7	
Er		0.006	0.055	0.35	12.0	0.65	37.2	
Yb	0.017	0.03	0.09	1.473	8.39	2.2	23.9	
Lu	0.014	0.033	0.092	1.617	5.5	2.25	20.2	

*Nash & Crecraft (1985).
†Arth (1976) and Pearce & Norry (1979).
‡Henderson (1982).

Table 5. *Parameters used in the modelling of 20% fractional melting plus 20% Rayleigh fractional crystallization of a TTG source to produce granitic rocks of the ABC in NE Afyon*

Trace element	D_0	C_0	20% fractional melting	D_0^1	C_0^1	20% fractional crystallization	Average of metagranitic rocks
Rb	0.425	63	110	0.315	110	128	94.6
Ba	1.804	717	439	1.295	439	411	592
Th	0.090	6.1	7.14	0.025	7.14	8.87	11.91
U	0.066	2.1	1.38	0.046	1.38	1.70	2.07
K	0.515	19093	30029	0.261	30029	35411	21252
Nb	0.789	7.1	8.47	0.200	8.47	10.12	11.81
Sr	9.195	473	62.8	1.549	62.8	55.5	55.2
Zr	0.572	152	225	0.089	225	275	251
Ti	0.804	2817	3319	0.700	3319	3549	4338
Y	0.788	17.3	20.7	0.378	20.7	27.7	26.4
La	0.492	26	42.0	0.212	42.0	50.0	28.0
Ce	0.528	45	70.0	0.243	70.0	82.6	66.5
Nd	0.707	18	23.2	0.341	23.2	26.9	24.9
Sm	1.050	3.50	3.37	0.361	3.37	3.88	5.18
Eu	1.752	0.95	0.59	1.338	0.59	0.58	1.10
Gd	1.177	3.0	2.63	0.315	2.63	3.06	4.68
Tb	0.104	0.49	0.69	0.111	0.69	0.84	0.76
Dy	0.835	3.50	4.01	0.307	4.01	4.68	4.27
Er	0.699	1.90	2.46	0.156	2.46	2.96	2.66
Yb	0.613	1.33	1.88	0.151	1.88	2.27	2.51
Lu	0.569	0.23	0.34	0.219	0.34	0.40	0.41

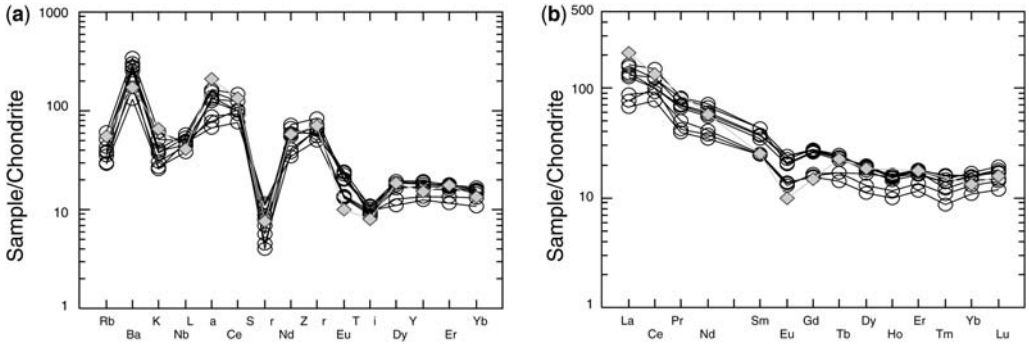

Fig. 9. (**a**) and (**b**) trace element and REE diagrams for the granitic rocks and their comparison with the calculated composition for 20% fractional melting plus 20% Rayleigh fractional crystallization of a TTG source. ○, granitic rocks; ◆, granitic rocks obtained from 20% fractional melting plus 20% Rayleigh fractional crystallization of the TTG source of Condie (2005).

includes quartz, microperthitic K-feldspar and microcline, with accessory minerals such as titanite, allanite, apatite and zircon. The granitic rocks in the latter locality contain alkali feldspar (disordered orthoclase), plagioclase (oligoclase–andesine in composition), quartz and biotite as relict phases. The accessory minerals are titanite, zircon, monazite, apatite and, rarely, opaque minerals.

Geochemically, the quartz porphyry rocks of Sandikli (Gürsu & Goncuoglu 2006) have higher SiO_2 (73.56–77.87 wt%), K_2O (4.73–7.81 wt%) and TiO_2 (0.16–0.48 wt%) and lower Al_2O_3 (11.68–13.68 wt%), Fe_2O_3 (1.05–3.38 wt%), P_2O_5 (0.02–0.13 wt%) and MgO (0.21–1.1 wt%) than the granitic rocks of NE Afyon (see Fig. 7). They can be clearly distinguished from the latter also by lower Y/Nb (2–5 ppm) and Ti/Zr (<11), higher REE abundances ($\sum$REE 220 ppm), lower $Eu/Eu^* = 0.16–0.33$, highly fractionated $(La/Yb)_N = 2.6–13.8$ and $(La/Sm)_N = 2.2–4.2$, and relatively flat $(Gd/Yb)_N = 0.9–1.9$ (for a brief review see Gürsu & Goncuoglu 2006). The granitic rocks, on the other hand, show relatively less enriched LREE and more depleted HREE patterns (see Fig. 8a and b). The correlative histogram

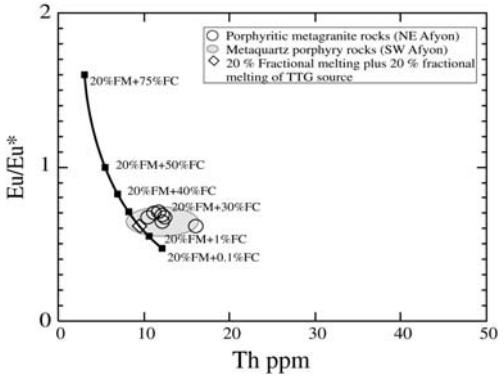

Fig. 10. Eu/Eu*–Th diagram (Kirstein *et al.* 2000) with calculated model curves for closed-system fractional crystallization. Modal curve was generated from 20% fractional partial melting of starting composition of TTG source of Condie (2005), where amounts of fractional crystallization (0.1–75%) are indicated.

Table 6. *Zircon and apatite saturation temperatures of the quartz porphyry rocks of the Geyikdağ unit in SW Afyon*

Sample no.	Zircon saturation temperature (°C)	Apatite saturation temperature (°C)
7	781	919
176	792	899
192	833	823
198	845	905
199	838	907
301	821	998
336	791	873
337A	783	925
344	804	881
664	844	947
692	811	970
740	807	959
744	832	952
745	839	975
944	807	886
1058	829	785
Average	816	912

The whole-rock analyses of the samples are from Gürsu & Goncuoglu (2006).

diagrams also indicate that on average the granitic rocks in the ABC of NE Afyon display Zr, Hf, Eu and Ti enrichments and Th, Nb, La, Ce, Nd, Sm, Gd, Tb, Dy, Y, Ho, Er, Tm, Ty and Lu depletions (Fig. 11a). Moreover, the Ti/Zr–Nb/Y, $\sum$REE–$(La/Yb)_N$ and Eu/Eu*–$(La/Yb)_N$ variation diagrams clearly reflect the presence of two chemically different felsic rock groups in the Late Neoproterozoic basements of the Geyik Dag and Kütahya-Bolkar Dagı units (Fig. 11b–d). Petrographical and geochemical characteristics suggest that the metaquartz porphyry rocks in Sandikli may represent the more felsic part of the coeval granitic magmatism that produced the granitic rocks in the NE Afyon area. Both rock types were formed from a TTG-type source by 20% fractional melting and 20% Rayleigh fractional crystallization (for a brief review see Gürsu & Goncuoglu 2006) in the upper continental crust.

A comparison of the Neoproterozoic felsic magmatism in the Kütahya–Bolkar Dagı (NE Afyon) and Geyik Dag (Sandikli) units in the Western Taurides is shown in Table 7.

Geodynamic implications and conclusions

The granitic rocks within the Late Neoproterozoic basement of the Taurides were ascribed to a post-collisional extension in the North Gondwanan margin (Goncuoglu 1996; Goncuoglu & Kozlu 2000; Gürsu *et al.* 2004*a*; Gürsu & Goncuoglu 2006). This event very probably followed the southward subduction of the oceanic lithosphere beneath the Gondwanan continental crust (e.g. see Gürsu & Goncuoglu 2005, fig. 13) that formed the 590 and 570 Ma arc-type granitoids intruding an older (890–710 Ma, Chen *et al.* 2002) sector of continental crust in the Safranbolu area of northern Turkey. The early Late Neoproterozoic rocks in northern Turkey were attributed to North Gondwana, are of tonalitic and granitic composition, and have low Nb/Y ratios and Ti contents, consistent with those of arc rocks (Chen *et al.* 2002). This tonalitic basement may be the TTG-type source of the Late Neoproterozoic granitic rocks in the Afyon and Sandikli areas. An alternative source for the studied granitoids may be the Mid-Proterozoic

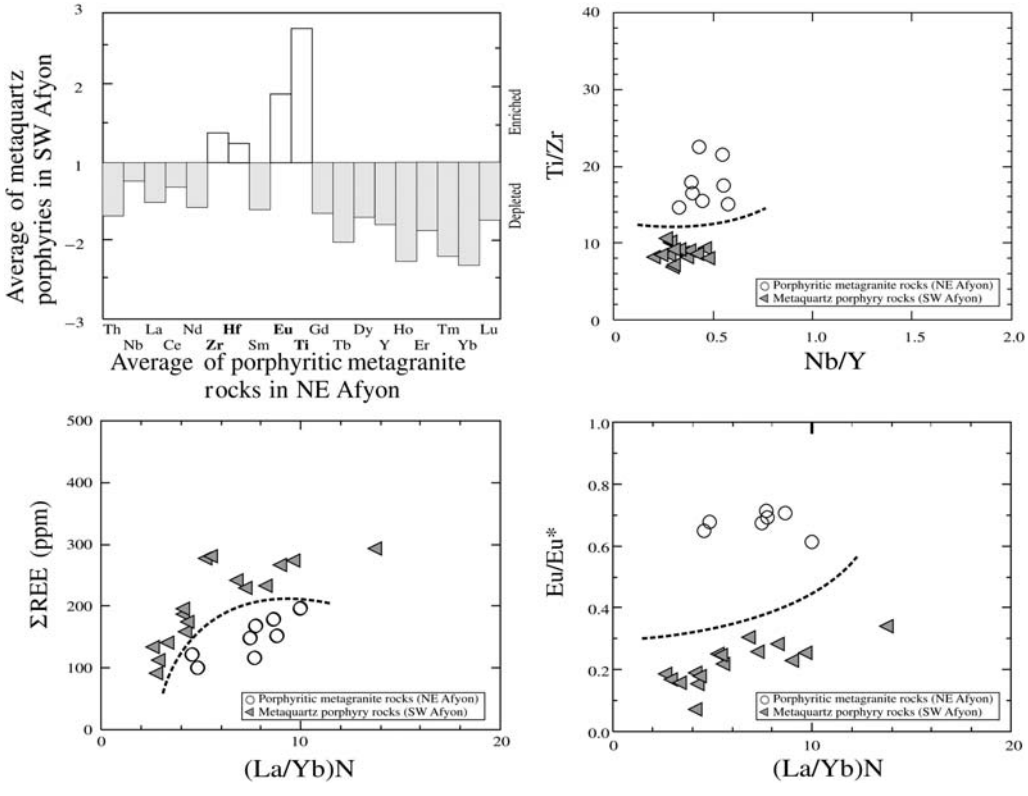

Fig. 11. (**a**) Correlative, (**b**) Ti/Zr–Nb/Y, (**c**) $\sum$REE–$(La/Yb)_N$ (from Zhao *et al.* 2004), (**d**) Eu/Eu*–$(La/Yb)_N$ variation diagrams indicating the differences between the granitic rocks in the Kütahya–Bolkar Dagı unit of NE Afyon (ABC) and quartz porphyry rocks of the Geyik Dag Unit of Sandikli, SW Afyon.

Table 7. *A comparison of the Neoproterozoic felsic magmatism in the Kütahya–Bolkar Dagı (NE Afyon) and Geyik Dağ (Sandıklı) units in the Western Taurides*

Feature	Kütahya–Bolkar Dağı (NE Afyon) Unit	Geyik Dağ (Sandıklı) Unit
Stratigraphy	The Late Neoproterozoic basement is unconformably overlain by Late Palaeozoic units and the Early Cambrian–Late Ordovician units are missing	The Late Neoproterozoic basement is unconformably overlain by Early Cambrian–Late Ordovician units. The Late Palaeozoic units are missing
Type of metamorphism	Multiple phases of tectonothermal events were observed as greenschist-facies (first), HP/LT blueschist-facies (350 °C and 6–9 kbar pressure, 30 km burial depths) (second) and greenschist-facies (third) overprints (Göncüoglu *et al.* 2001; Candan *et al.* 2005)	Multiple phases of tectonothermal events were observed as pre-Early Cambrian low-grade dynamothermal metamorphism (*c*. 300 °C, 4.2 kbar pressure, *c*. 15 km burial depths) and Late Palaeozoic very low grade metamorphism (3.2 kbar pressure, *c*. 10 km burial depth)
Felsic magmatism		
Nature	Metamorphosed leucogranitic rocks and sills or dykes of porphyry rocks	Meta-rhyolites and irregularly distributed sills or dykes of meta-quartz porphyries
Mineral contents	Alkali feldspar, plagioclase (oligoclase–andesine in composition), biotite, titanite, zircon, monazite, apatite and, rarely, opaque minerals	Quartz, microperthitic orthoclase, microcline with minor amount of biotite, titanite, allanite, apatite, zircon and opaque minerals
Geochemical fingerprints	Sub-alkaline (peraluminous). Magmatic differentiation by fractional crystallization is the main factor in formation of the leucogranitic rocks. Trace element and REE patterns show distinctive depletion in Rb, K, Nb, Sr, P and Ti, and slight enrichment in Ba, Th, La, Ce, Nd, Zr	Sub-alkaline and cogenetic. The role of the fractional crystallization is consistent with the fractionation of an assemblage of plagioclase, alkali feldspar and iron oxides. The trace element patterns show depletion in Nb, Sr, P and Ti and enrichment in Th, U, La, Ce, Nd, Sm and Zr
Melting process	Low H_2O activity, TTG dehydration	Low H_2O activity, granite and felsic rock dehydration
Source	I-type (Proterozoic TTG)	I-type (Proterozoic granites or felsic rocks)
P–T conditions during melting	Lower than 10 kbar, 800–850 °C	Lower than 10 kbar, 780–845 °C
Timing of emplacement (zircon ages)	541.1 ± 3.6 Ma (^{207}Pb–^{206}Pb) in leucogranitic rocks (this study)	543 ± 7 Ma (^{207}Pb–^{206}Pb) in meta-quartz porphyry rocks (Kröner & Şengör 1990), 541.3 ± 10.9 Ma (^{207}Pb–^{206}Pb) in meta-rhyolites (Gürsu & Göncüoglu 2006)
Associated deformation	Synkinematic S_1, S_2 and S_3 discrete crenulation cleavage is well developed	Synkinematic S_1, S_2 and S_3 discrete crenulation cleavage is well developed
Geodynamic model	Post-collisional extension, crustal thinning	Post-collisional extension, crustal thinning

(U–Pb single-zircon and SHRIMP ages; Anders *et al.* 2006) arc-related rocks recently reported from the orthogneisses in the Pelagonian basement in Greece, which were also attributed to a Gondwanan terrane (the Florina Terrane of Anders *et al.* 2006). As indicated by many workers (e.g. Condie 1981, 2005; Martin 1988, 1999; Martin *et al.* 2005), TTG magmas were derived from subducted basaltic crust in most Archaean cratonic terranes. The TTG-type melting of such a crustal source by post-collisional extension or lithospheric delamination after subduction of the oceanic lithosphere may have resulted in the formation of the Late Neoproterozoic post-collisional granitoids in the basement of the Taurides. This geodynamic scenario is in good agreement with models for various Peri-Gondwanan terranes (e.g. Murphy *et al.* 2002; Nance *et al.* 2002). Based on these similarities, Gürsu & Goncuoglu (2001, 2006) suggested that this magmatic activity in the Taurides should be considered as the eastern counterpart of the Cadomian magmatism.

Despite the differences in their post-Cadomian history (Variscan(?) and Alpine events) the geochemical comparison of the granitic rocks in the basements of two tectonic units (Geyik Dag and Kütahya-Bolkar Dagı units) in the Taurides has revealed the presence of two chemically different but genetically linked groups. In very general terms, it can be assumed that the rocks represent the products of more evolved end-members of the same parent magma. However, the present data are not sufficient to allow us speculate on details of the magmatic evolution; detailed radiometric age dating coupled with further geochemical evaluation of associated metaigneous rocks may in obtaining a better understanding of the relations.

To conclude, the recent petrological work on the granitic rocks in the Kütahya–Bolkar Dagı tectonic unit of the Taurides has revealed the following results.

(1) The Cadomian felsic magmas of the Kütahya–Bolkar Dagı unit were mostly emplaced between 545 and 540 Ma and they are believed to have been intruded during post-collisional stages of Cadomian orogeny. The mineralogical, petrographic and geochemical features of the porphyritic granitoids in the ABC indicate a sub-alkaline (peraluminous) nature. They have geochemical characteristics of I-type felsic intrusive rocks. It is suggested that fractional crystallization was the main differentiation process during the formation of these rocks.

(2) The low to very low unfractionated HREE and Y abundances in the granitic rocks suggest that the felsic magmas were evolved through the second-stage melting of a TTG source during intracrustal melting without residual garnet. Their trace element and REE patterns show distinctive depletion in Rb, K, Nb, Sr, P and Ti and slightly enrichment in Ba, Th, La, Ce, Nd and Zr, with fractionated $(La/Yb)_N$ and $(La/Sm)_N$, and relatively flat $(Gd/Yb)_N$ patterns. They display very similar patterns to a TTG source. The petrogenetic modelling and magmatic temperature studies also imply that the protoliths of the granitic rocks of the ABC were derived by partial melting of a TTG source by 20% fractional melting plus 20% Rayleigh fractional crystallization. This was achieved under <10 kbar pressure and water-undersaturated conditions. The felsic magma temperatures determined (*c.* 800–850 °C) are in general agreement with values from experimental studies (e.g. Clemens *et al.* 1986; Skjerlie & Johnston 1992; Patiño-Douce 1997) and support the model that I-type granites may be produced by partial melting of a tonalitic source.

(3) We propose that the felsic magmas were generated by crustal extension related to the Cadomian post-collisional magmatism. Therefore they represent the eastern equivalents of the Late Pan-African–Cadomian granitoids in North Africa and Gondwana-derived terranes in Southern and Central Europe (e.g. Chantraine *et al.* 2001; El-Nisr *et al.* 2001; Pin *et al.* 2002; Dörr *et al.* 2002; Mushkin *et al.* 2003).

(4) The ABC-type basement of the Kütahya–Bolkar Dagı unit and the Sandikli-type basement of the Geyik Dag unit are part of the same Cadomian terrane and the present differences in stratigraphy and metamorphism are due to subsequent (Variscan and Alpine) geological events.

This research was financially supported by General Directorate of Mineral Research and Exploration (MTA) and State Planning Organisation of the Republic of Turkey (MTA/DPT Project 2004-16B37). The authors gratefully acknowledge the comments of H. Kozlu and N. Turhan. We would like to thank M. Satır for help with Pb–Pb geochronological analyses at the Tübingen University, Laboratory of Geochronology. Special thanks go to S. Köksal for comments on the zircon typology and morphology. N. Ilbeyli, R. Kerrich and J. P. Liégeois are thanked for careful reviews and constructive editing.

References

ALLÈGRE, C. J. & BEN OTHMAN, D. 1980. Nd–Sr isotopic relationship in granitoid rocks and continental crust development: A chemical approach to orogenesis. *Nature*, **286**, 335–342.

ANDERS, B., REISCHMANN, T., KOSTOPOULOS, D. & POLLER, U. 2006. The oldest rocks of Greece: first evidence for a Precambrian terrane within the Pelagonian Zone. *Geological Magazine*, **143**, 41–58.

ARTH, J. G. 1976. Behaviour of trace elements during magmatic process—a summary of theoretical models

and their applications. *Journal of Research of the US Geological Survey*, **4**, 41–47.

BALLÈVRE, M., LE GOFF, E. & HÉBERT, R. 2001. The tectonothermal evolution of the Cadomian belt of northern Brittany, France: a Proterozoic volcanic arc. *Tectonophysics*, **331**, 19–43.

BANDRES, A., EGUILUZ, L., GIL IBARGUCHI, I. J. & PALACIOS, T. 2002. Geodynamic evolution of a Cadomian arc region: the northern Ossa–Morena zone, Iberian massif. *Tectonophysics*, **352**, 105–120.

BEARD, J. S. & LOFGREN, G. E. 1989. Effect of water on the composition of partial melts of greenstone and amphibolites at 1, 3 and 6.9 kb. *Science*, **244**, 195–197.

BEARD, J. S. & LOFGREN, G. E. 1991. Dehydration melting and water-saturated melting of basaltic and andesitic greenstone and amphibolites at 1, 3 and 6.9 kb. *Journal of Petrology*, **32**, 365–401.

CANDAN, O., DORA, O. Ö., OBERHANSLI, R., CETINKAPLAN, M., PARTZCH, J. H., WARKUS, F. C. & DÜRR, S. 2001. Pan-African high-pressure metamorphism in the Precambrian basement of the Menderes Massif, western Anatolia, Turkey. *International Journal of Earth Sciences*, **89**, 793–811.

CANDAN, O., OBERHANSLI, R., ÇETINKAPLAN, M., RIMMELÉ, G. & AKAL, C. 2003. Regional occurrence of Fe–Mg carpholite in Triassic metasediments of Afyon Zone, Turkey: implications for metamorphic evolution. *In*: DORA, O. Ö. (ed.) *Proceedings of 56th National Geological Congress of Turkey*, *Chamber of Turkish Geological Engineers, Ankara*, 57–59.

CANDAN, O., ÇETINKAPLAN, M., OBERHANSLI, R., RIMMELÉ, G. & AKAL, C. 2005. Alpine high-*P*/low-*T* metamorphism of the Afyon Zone and implication for the metamorphic evolution of Western Anatolia, Turkey. *Lithos*, **84**, 102–124.

CHANTRAINE, J., EGAL, E., THIEBLEMONT, D., LE GOFF, E., GUERROT, C., BALLÈVRE, M. & GUENNOC, P. 2001. The Cadomian active margin (North Armorican Massif, France): a segment of the North Atlantic Pan-African belt. *Tectonophysics*, **331**, 1–18.

CHAPPELL, B. W. 1999. Aluminium saturation in I- and S-type granites and the characterization of fractionated haplogranites. *Lithos*, **46**, 535–551.

CHEN, F., SIEBEL, W., SATIR, M. & TERZIOGLU, M. N. 2002. Geochronology of Karadere basement (NW Turkey) and implications for the geological evolution of the İstanbul zone. *International Journal of Earth Sciences*, **91**, 469–481.

CLEMENS, J. D. & VIELZEUF, D. 1987. Constraints on melting and magma production in the crust. *Earth and Planetary Science Letters*, **86**, 287–306.

CLEMENS, J. D., HOLLOWAY, J. R. & WHITE, A. J. R. 1986. Origin of an A-type granite: experimental constraints. *American Mineralogist*, **71**, 317–324.

COLLINS, W. J., BEAMS, S. D., WHITE, A. J. R. & CHAPPELL, B. W. 1982. Nature and origin of A-type granites, with particular reference to south-eastern Australian. *Contributions to Mineralogy and Petrology*, **80**, 189–200.

CONDIE, C. K. 1981. *Archaean Greenstone Belts.* Elsevier, Amsterdam.

CONDIE, C. K. 1993. Chemical composition and evolution of the upper continental crust: contrasting results from surface samples and shales. *Chemical Geology*, **104**, 1–37.

CONDIE, C. K. 2005. TTGs and adakites: are they both slab melts? *Lithos*, **80**, 33–44.

DAVIES, G. R. & MACDONALD, R. 1987. Crustal influence in the petrogenesis of the Naivasha basalt–comendite complex: combined trace elements and Sr–Nd–Pb isotope constraints. *Journal of Petrology*, **28**, 1009–1031.

DORA, O. Ö., CANDAN, O., DÜRR, S. & OBERHANSLI, R. 1995. New evidence on the geotectonic evolution of the Menderes Massif. *In*: PISKIN, Ö., AKGUN, M., SAVASCIN, M. Y. & TARCAN, G. (eds) *International Earth Science Colloquium on the Aegean Region, Proceedings,* 9 Eylül University, İzmir, Turkey, V-I, 53–72.

DÖRR, W., ZULAUF, G., FIALA, J., FRANKE, W. & VEJNAR, Z. 2002. Neoproterozoic to Early Cambrian history of an active plate margin in the Tepla–Barrandian unit—a correlation of U–Pb isotopic-dilution–TIMS ages (Bohemia, Czech Republic). *Tectonophysics*, **352**, 65–85.

EGAL, E., GUERROT, C., LE GOFF, D., THIÉBLEMONT, D. & CHANTRAINE, J. 1996. The Cadomian orogeny revisited in northern France. *In*: NANCE, R. D. & THOMPSON, M. D. (eds) *Avalonian and Related Peri-Gondwanan Terranes of the Circum-North Atlantic.* Geological Society of America, Special Papers, **304**, 281–318.

EGAL, E., THIÉBLEMONT, D., LAHONDÉRE, D. *ET AL.* 2002. Late Eburnean granitization and tectonics along the western and northwestern margin of the Archean Kénéma–Man domain (Guinea, West African Craton). *Precambrian Research*, **117**, 57–84.

EL-NISR, S. A., EL-SAYED, M. M. & SALEH, G. M. 2001. Geochemistry and petrogenesis of Pan-African late to post orogenic younger granitoids at Shalatin–Halaib, South Eastern Desert, Egypt. *Journal of African Earth Sciences*, **33**, 261–282.

GENNA, A., NEHLIG, P., LE GOFF, E., GUERROT, C. & SHANTI, M. 2002. Proterozoic tectonism of the Arabian Shield. *Precambrian Research*, **117**, 21–40.

GONCUOGLU, M. C. 1996. Terranes with contrasting pre-Lower Palaeozoic basement rocks in NW Gondwana: geodynamic implications. *Revista Yacimiento Petroliferos Fiscales Bolivianos*, **17**, 475–476.

GONCUOGLU, M. C. & KOZLU, H. 2000. Early Palaeozoic evolution of the NW Gondwanaland: data from southern Turkey and surrounding regions. *Gondwana Research*, **3**, 315–323.

GONCUOGLU, M. C., ÖZCAN, A., TURHAN, N. & IŞIK, A. 1992. *Stratigraphy of the Kütahya region. A geotraverse across suture zones in NW Anatolia.* General Directorate of Mineral Research and Exploration, Special Publications, **1**, 3–8.

GONCUOGLU, M. C., DIRIK, K. & KOZLU, H. 1997. General characteristics of pre-Alpine and Alpine Terranes in Turkey: explanatory notes to the terrane map of Turkey. *Annales Géologiques des Pays Hellénique*, **37**, 515–536.

GONCUOGLU, M. C., TURHAN, N. & TEKIN, U. K. 2003. Evidence for the Triassic rifting and opening of the Neotethyan Izmir–Ankara Ocean and discussion on

the presence of Cimmerian events at the northern edge of the Tauride–Anatolide Platform, Turkey. *Bollettino Società Geologica Italiana*, Volume Speciale, **2**, 203–212.

GÜRSU, S. & GONCUOGLU, M. C. 2001. Characteristic features of the Late Precambrian felsic magmatism in Western Anatolia: implications for the Pan-African evolution in NW PeriGondwana. *Gondwana Research*, **4**, 169–170.

GÜRSU, S. & GONCUOGLU, M. C. 2005. Early Cambrian back-arc volcanism in the western Taurides, Turkey: implications for rifting along the northern Gondwanan margin. *Geological Magazine*, **142**, 617–631.

GÜRSU, S. & GONCUOGLU, M. C. 2006. Petrogenesis and tectonic setting of Cadomian felsic igneous rocks, Sandıklı area of the western Taurides, Turkey. *International Journal of Earth Sciences*, **95**, 741–757.

GÜRSU, S., KOZLU, H., GONCUOGLU, M. C. & TURHAN, N. 2003. Correlation of the basement rocks and lower Palaeozoic covers of the western part of the Central Taurides. *Turkish Association of Petroleum Geologist Bulletin*, **15**, 129–153 [in Turkish].

GÜRSU, S., GONCUOGLU, M. C. & BAYHAN, H. 2004*a*. Geology and geochemistry of the pre-Early Cambrian rocks in Sandıklı area: implications for the Pan-African evolution in NW Gondwanaland. *Gondwana Research*, **7**, 923–935.

GÜRSU, S., GONCUOGLU, M. C., TURHAN, N. & KOZLU, H. 2004*b*. Characteristic features of Precambrian, Palaeozoic and Lower Mesozoic successions of two different tectono-stratigraphic units of the Taurides in Afyon area, western Central Turkey. *In*: CHATZIPETROS, A. & PAVLIDES, S. B. (eds) *5th International Symposium on Eastern Mediterranean Geology Proceedings*, Aristotle University, Thessaloniki, Greece, 80–83.

HARRISON, M. T. & WATSON, B. E. 1984. The behaviour of apatite during crustal anatexis: Equilibrium and kinetic considerations. *Geochimica et Cosmochimica Acta*, **48**, 1467–1477.

HELZ, R. T. 1976. Phase relations of basalts in their melting ranges at $P_{H2O} = 5$ kb. Part II. Melt composition. *Journal of Petrology*, **17**, 139–193.

HETZEL, R. & REISCHMANN, T. 1996. Intrusion age of Pan-African augen-gneisses in the southern Menderes Massif and the age of cooling after Alpine ductile extensional deformation. *Geological Magazine*, **33**, 565–572.

HENDERSON, P. 1982. *Inorganic Geochemistry*. Pergamon, Oxford.

HILDRETH, W. 1981. Gradients in silicic magma chambers: implications for lithospheric magmatism. *Journal of Geophysical Research*, **86**, 10153–10192.

HIRDES, W. & DAVIS, D. W. 2002. U–Pb geochronology of Palaeoproterozoic rocks in the southern part of the Kedougou–Kéniéba inlier, Senegal, West Africa: Evidence for diachronous accretionary development of the Eburnean province. *Precambrian Research*, **118**, 83–99.

KIRSTEIN, A. L., PEATE, W. P., HAWKESWORTH, J. C., TURNER, P. S., HARRIS, C. & MANTOVANI, M. S. M. 2000. Early Cretaceous basaltic and rhyolitic magmatism in southern Uruguay associated with the opening of the South Atlantic. *Journal of Petrology*, **41**, 1423–1438.

KOBER, B. 1986. Whole-grain evaporations for ^{207}Pb–^{206}Pb age investigations on single zircons using a double-filament thermal ion source. *Contributions to Mineralogy and Petrology*, **93**, 482–490.

KORALAY, E., DORA, O. Ö., CHEN, F., SATIR, M. & CANDAN, O. 2004. Geochemistry and geochronology of orthogneisses in the Derbent (Alaşehir) area, eastern part of Ödemiş–Kiraz submassif, Menderes Massif: Pan-African magmatic activity. *Turkish Journal of Earth Science*, **13**, 37–61.

KOZLU, H. & GONCUOGLU, M. C. 1997. Stratigraphy of the Infracambrian rock-units in the Eastern Taurides and their correlation with similar units in Southern Turkey. *In*: GONCUOGLU, M. C. & DERMAN, A. S. (eds) *Early Palaeozoic in NW Gondwana*. Turkish Association Petroleum Geologists, Special Publications, **3**, 50–61.

KRÖNER, A. & SENGÖR, A. M. C. 1990. Archean and Proterozoic ancestry in the Late Precambrian to Early Palaeozoic crustal elements of southern Turkey as revealed by single zircon dating. *Geology*, **18**, 1186–1190.

LEAT, P. T., JACKSON, S. E., THORPE, R. S. & STILLMAN, C. T. 1986. Geochemistry of bimodal basalt–subalkaline/peralkaline rhyolite provinces within the Southern British Caledonides. *Journal of the Geological Society, London*, **143**, 259–273.

LIÉGEOIS, J. P., BERZA, T., TATU, M. & DUCHESNE, J. C. 1996. The Neoproterozoic Pan-African basement from the Alpine Lower Danubian nappe system (South Carpathians, Romania). *Precambrian Research*, **80**, 281–301.

LIEW, T. C. & MCCULLOCH, M. T. 1985. Genesis of granitoid batholiths of Peninsular Malaysia and implications for models of crustal evolution: evidence from a Nd–Sr isotopic and U–Pb zircon study. *Geochimica et Cosmochimica Acta*, **49**, 587–600.

LINNEMANN, U. & ROMER, R. L. 2002. The Cadomian orogeny in Saxo-Thuringia, Germany. Geochemical and Nd–Sr–Pb isotopic characterization of marginal basins with constraints to geotectonic setting and provenance. *Tectonophysics*, **352**, 33–64.

LINNEMANN, U., GEHMLICH, M., TICHOMIROWA, M. *ET AL*. 2000. From Cadomian subduction to early Palaeozoic rifting: the evolution of Saxo-Thuringia at the margin of Gondwana in the light of single zircon geochronology and basin development (Central European Variscides, Germany). *In*: FRANKE, W., HAAK, V., ONCKEN, O. & TANNER, D. (eds) *Orogenic Processes: Quantification and Modelling in the Variscan Belt of Central Europe.* Geological Society, London, Special Publications, **179**, 131–153.

LINNEMANN, U., MCNAUGHTON, N. J., ROMER, R. L., GEHMLICH, M., DROST, K. & TONK, C. 2004. West African provenance for Saxo-Thuringia (Bohemian Massif): Did Armorica ever leave pre-Pangean Gondwana?—U/Pb-SHRIMP zircon evidence and the Nd-isotopic record. *International Journal of Earth Sciences*, **93**, 683–705.

LOOS, S. & REISCHMANN, T. 1999. The evolution of the southern Menderes Massif in SW Turkey as revealed

by zircon dating. *Journal of Geological Society, London*, **156**, 1021–1030.

MARTIN, H. 1988. Archaean and modern granitoids as indicators of changes in geodynamic processes. *Revista Brasileira de Geociencias*, **17**, 360–365.

MARTIN, H. 1999. The adakitic magmas: modern analogues of Archaean granitoids. *Lithos*, **46**, 411–429.

MARTIN, H., SMITHIES, R. H., RAPP, R., MOYEN, J. F. & CHAMPION, D. 2005. An overview of adakite, tonalite–trondhjemite–granodiorite (TTG), and sanukitoid: relationships and some implications for crustal evolution. *Lithos*, **79**, 1–24.

MINGRAM, B., KRÖNER, A., HEGNER, E. & KRENTZ, O. 2004. Zircon ages, geochemistry, and Nd isotopic systamatics of pre-Variscan orthogneisses from the Erzgebirge, Saxony (Germany), and geodynamic interpretation. *International Journal of Earth Sciences*, **93**, 706–727.

MONTEL, J. M. 1993. A model for monazite/melt equilibrium and the applications to the generation of granitic magmas. *Chemical Geology*, **110**, 127–146.

MURPHY, J. B., EGUILUZ, L. & ZULAUF, G. 2002. Cadomian Orogens, peri-Gondwanan correlatives and Laurentia–Baltica connections. *Tectonophysics*, **352**, 1–9.

MURPHY, J. B., PISAREVSKY, S. A., NANCE, R. D. & KEPPIE, J. D. 2004. Neoproterozoic–Early Palaeozoic evolution of peri-Gondwanan terranes: implications for Laurentia–Gondwana connections. *International Journal of Earth Sciences*, **93**, 659–682.

MUSHKIN, A., NAVON, O., HALICZ, L., HARTMANN, G. & STEIN, M. 2003. The petrogenesis of A-type magmas from the Amram massif, Southern Israel. *Journal of Petrology*, **44**, 815–832.

NANCE, R. D., MURPHY, J. B., KEPPIE, J. D. & O'BRIEN, S. J. 2002. A Cordilleran model for the evolution of Avalonia. *Tectonophysics*, **352**, 11–31.

NASH, W. P. & CRECRAFT, H. R. 1985. Partition coefficient for trace elements in silicic magmas. *Geochimica et Cosmochimica Acta*, **49**, 2309–2322.

NEUBAUER, F. 2002. Evolution of late Neoproterozoic to early Palaeozoic tectonic elements in Central and Southeast European Alpine mountain belts: review and synthesis. *Tectonophysics*, **352**, 87–103.

ÖZCAN, A., GONCUOGLU, M. C. & TURHAN, N. 1989. *The geology of Kütahya, Cifteler, Bayat and Ihsaniye area*. Mineral Research and Exploration General Directorate Report, **8974**.

PATIÑO-DOUCE, A. E. 1997. Generation of metaaluminous A-type granites by low-pressure melting of calc-alkaline granitoids. *Geology*, **25**, 743–746.

PATIÑO, M. L. G. & PATIÑO-DOUCE, A. E. 1987. Petrologia y petrogénesis del Batolito de Achala, provincial de Córdoba, a la luz de la evidencia de campo. *Revista de la Asociación Geológica Argentina*, **42**, 201–205.

PATOČKA, F. & ŠTORCH, P. 2004. Evolution of geochemistry and depositional settings of Early Palaeozoic siliciclastics of the Barrandian (Teplá–Barrandian Unit, Bohemian Massif, Czech Republic). *International Journal of Earth Sciences*, **93**, 728–741.

PEARCE, J. A. & NORRY, M. J. 1979. Petrogenetic implication of Ti, Zr, Y and Nb variations in volcanic rocks. *Contributions to Mineralogy and Petrology*, **69**, 33–47.

PECCERILLO, A. & TAYLOR, S. R. 1976. Geochemistry of Eocene calcalkaline volcanic rocks from the Kastamonu area, northern Turkey. *Contributions to Mineralogy and Petrology*, **58**, 63–81.

PICCOLI, P. M. & CANDELA, P. A. 1994. Apatite in felsic rocks, a model for the estimation of initial halogen concentrations in the Bishop Tuff (Long Walley) and Tuolumne intrusive suite (Sierra Nevada Batholith) magmas. *American Journal of Science*, **294**, 92–135.

PICCOLI, P. M., CANDELA, P. A. & WILLIAMS, T. J. 1999. Estimation of aqueous HCl^- and Cl^- concentrations in felsic systems. *Lithos*, **46**, 591–604.

PICHAVANT, M., MONTEL, J. M. & RICHARD, L. R., 1992. Apatite solubility in peraluminous liquids: experimental data and an extension of the Harrison–Watson model. *Geochimica et Cosmochimica Acta*, **56**, 3855–3861.

PIN, C., LINÁN, E., PASCUAL, E., DONAIRE, T. & VALENZUELA, A. 2002. Late Proterozoic crustal growth in the European Variscides: Nd isotope and geochemical evidence from the Sierra de Cordoba andesites (Ossa–Morena Zone, southern Spain). *Tectonophysics*, **352**, 133–151.

PUPIN, J. P. 1980. Zircon and granite petrology. *Contributions to Mineralogy and Petrology*, **73**, 207–220.

RUTTER, M. J. & WYLLIE, P. J. 1988. Melting of vapour-absent tonalite at 10 kbar to simulate dehydration melting in the deep crust. *Nature*, **331**, 159–160.

SING, J. & JOHANNES, W. 1996*a*. Dehydration melting of tonalities. Part I. Beginning of melting. *Contributions to Mineralogy and Petrology*, **125**, 16–25.

SING, J. & JOHANNES, W. 1996*b*. Dehydration melting of tonalities. Part II. Composition of melting and solids. *Contributions to Mineralogy and Petrology*, **125**, 26–44.

SKJERLIE, K. P. & JOHNSTON, A. D. 1992. Fluid-absent melting behaviour of and F-rich tonalitic gneiss at mid-crustal pressures: implications for the generation of anorogenic granites. *Journal of Petrology*, **34**, 785–815.

SPULBER, S. D. & RUTHERFORD, M. J. 1983. The origin of rhyolite and plagiogranite in oceanic crust: an example study. *Journal of Petrology*, **24**, 1–25.

STRACHAN, R. A., D'LEMOS, R. S. & DALLMEYER, R. D., 1996. Late Precambrian evolution of an active plate margin: North Armorican Massif, France. *In*: NANCE, R. D. & THOMPSON, M. D. (eds) *Avalonian and Related Peri-Gondwanan Terranes of the Circum-North Atlantic*. Geological Society of America, Special Papers, **304**, 319–332.

SUN, S. S. & MCDONOUGH, W. F. 1989. Chemical and isotopic systematics of oceanic basalts: implications for mantle composition and processes. *In*: SAUNDERS, A. D. & NORRY, M. J. (eds) *Magmatism in the Ocean Basins*. Geological Society, London, Special Publications, **42**, 313–345.

TAYLOR, S. R. & MCLENNAN, S. M. 1995. The geochemical evolution of the continental crust. *Reviews of Geophysics*, **33**, 241–265.

THOMSON, A. B. 1996. Fertility of crustal rocks during anatexis. *Transactions of the Royal Society of Edinburgh*, *Earth Sciences*, **87**, 1–10.

USTAÖMER, P. A., MUNDIL, R. & RENNE, P. R. 2005. U–Pb and Pb–Pb zircon ages for arc-related intrusions of the Bolu Massif (W Pontides, NW Turkey): evidence for Late Precambrian (Cadomian) age. *Terra Nova*, **17**, 215–223.

VAVRA, G., GEBAUER, D., SCHMID, R. & COMPSTON, W. 1996. Multiple zircon growth and recrystallization during polyphase late Carbonifereous to Triassic metamorphism in granulites of the Ivrea Zone (Southern Alps): an ion microprobe (SHRIMP) study. *Contributions to Mineralogy and Petrology*, **122**, 337–358.

VIELZEUF, D. & MONTEL, J. M. 1992. Experimental determination of fluid-absent melting of a natural quartz-rich metagreywacke, 1. phase relations. *Terra Abstracts*, **3**, 30.

WATSON, B. E. & HARRISON, M. T. 1983. Zircon saturation revisited: temperature and composition effects in a variety of crustal magma types. *Earth and Planetary Science Letters*, **64**, 295–304.

WINCHESTER, J. A. & FLOYD, P. A. 1976. Geochemical magma type discrimination: application to altered and metamorphosed basic igneous rocks. *Earth and Planetary Science Letters*, **28**, 459–469.

WINCHESTER, J. A. & FLOYD, P. A. 1977. Geochemical discrimination of different magma series and their differentiation products using immobile elements. *Chemical Geology*, **20**, 325–343.

WINTHER, K. T. & NEWTON, R. C. 1991. Experimental melting of hydrous low-K tholeiite: evidence on the origin of Archaean craton. *Bulletin of the Geological Society of Denmark*, **39**, 213–228.

WOLF, M. B. & WYLLIE, P. J. 1994. Dehydration melting of amphibolites at 10 kbar: the effects of temperature and time. *Contributions to Mineralogy and Petrology*, **115**, 369–383.

ZENG, L., ASIMOW, D. P. & SALEEBY, J. B. 2005. Coupling of anatectic reactions and dissolution of accessory phases and the Sr and Nd isotope systematics of anatectic melts from a metasedimentary source. *Geochimica et Cosmochimica Acta*, **64**, 3671–3682.

ZHAO, J. H., HU, R. & LIU, S. 2004. Geochemistry, petrogenesis and tectonic significance of Mesozoic mafic dykes, Fujian Province, Southeastern China. *International Geology Review*, **46**, 542–557.